Aminopropylimidazole and Its Zinc Complex: CO_2 Chemistry and Catalytic Synthesis of Cyclic Carbonates

Feda'a M. Al-Qaisi,[a] Abdussalam K. Qaroush,[b*] Ahmad M. Ala'mar,[a] Ala'a F, Eftaiha,[a*] Khaleel I. Assaf, [c*] and Timo Repo[a,d]*

[a] Department of Chemistry, Faculty of Science, The Hashemite University, Zarqa 13133, Jordan
[b] Department of Chemistry, Faculty of Science, The University of Jordan, Amman 11942, Jordan
[c] Department of Chemistry, Faculty of Science, Al-Balqa Applied University, Al-Salt 19117, Jordan
[d] Department of Chemistry, University of Helsinki, A.I. Vertasin aukio 1, 00014 Helsinki, Finland
Corresponding authors E-mail: fedam@hu.edu.jo, a.qaroush@ju.edu.jo, alaa.eftaiha@hu.edu.jo, khaleel.assaf@bau.edu.jo

Electronic Supplementary Information

Table of Content

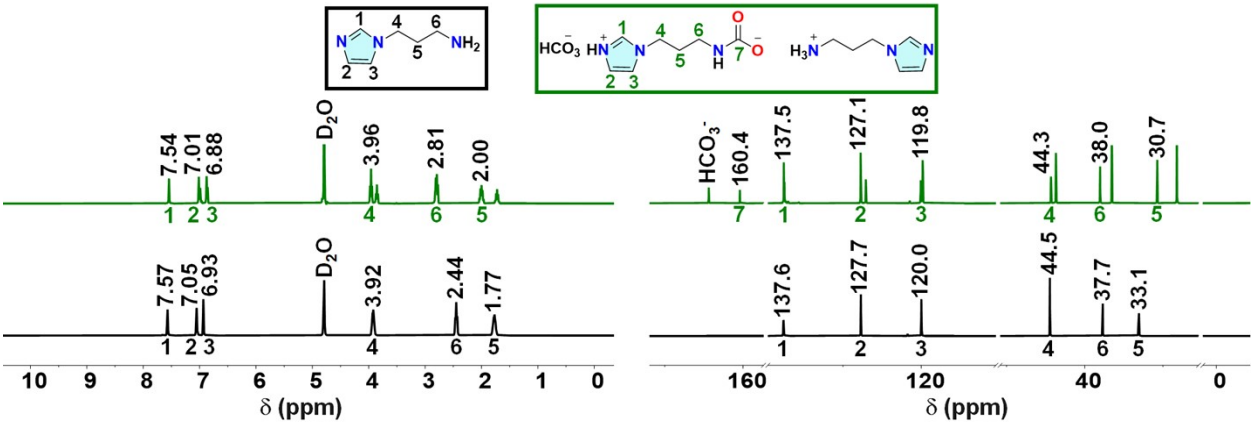

Figure S1. $^{1}H/^{13}C$ NMR spectra in D_2O of api (black color) and api-CO_2 adduct (green color)

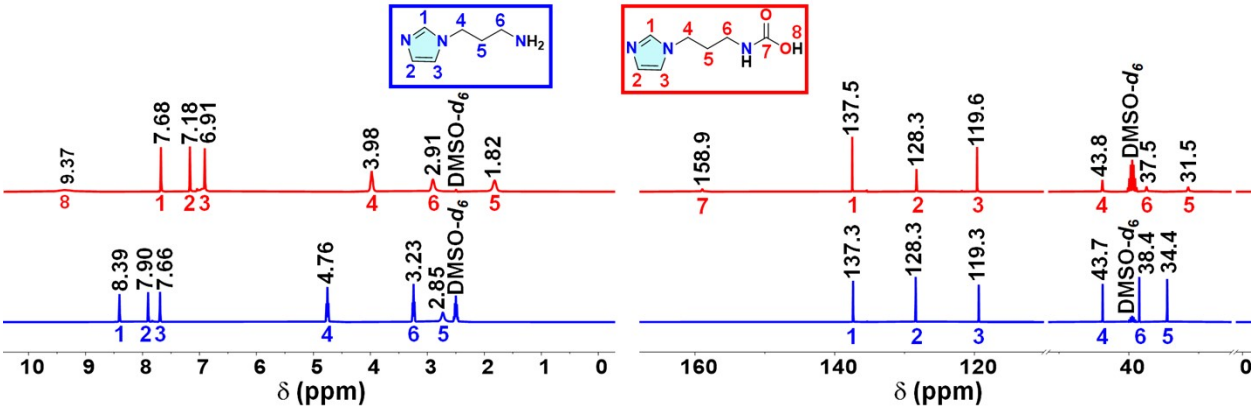

Figure S2. $^{1}H/^{13}C$ NMR spectra in DMSO-d_6 of api (blue color) and api-CO_2 adduct (red color)

1. Effect of Thermal Heating on Api-CO_2

The thermal stability of the CO_2 adducts formed between the unbound api and CO_2 in both D_2O and DMSO- solvents were explored. The investigation involved heating solutions to 80 ºC and measuring the NMR spectra at three-time intervals for 45 min. **Figure S3** illustrates the changes observed in the spectra. We see an increase in signal intensity corresponding to HCO_3^- and a decrease in the signal intensity associated with the carbamate group (labelled as C7). This suggests that the carbamate species is less stable in D_2O. Furthermore, the solution color changed from pale yellow to bright pink, ultimately reaching a persistent dark pink color (**Figure S4**).

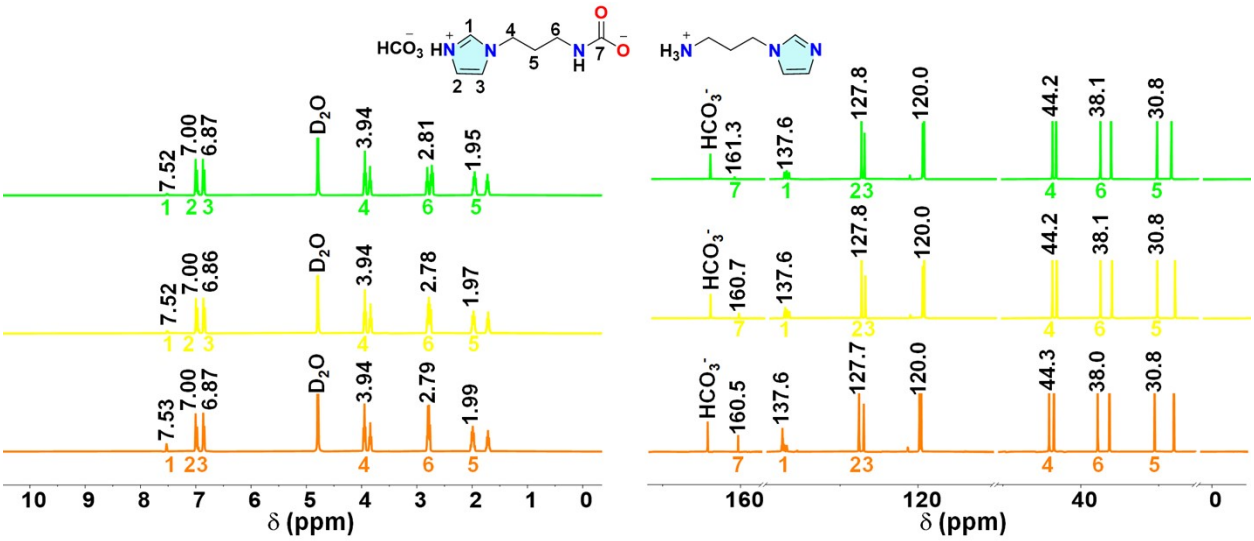

Figure S3. Stacked $^{1}H/^{13}C$ NMR spectra of the api-CO_2 adduct in D_2O, measured at 15, 30, and 45 min (orange, yellow, and green colors) after thermal heating at 80 °C

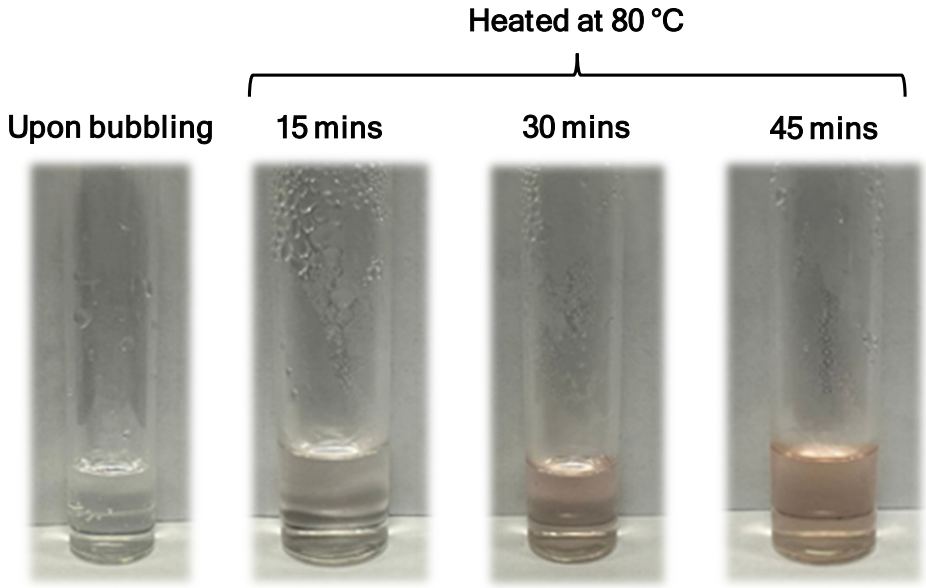

Figure S4. Photographs of api-CO_2 in D_2O showing color transition during heating, from pale yellow to bright pink, and finally to a persistent dark pink

In contrast to the D_2O scenario, heating the api-CO_2 adduct in DMSO- reveals a different thermal response. The ^{1}H NMR measurements suggest the occurrence of proton shuttling between the oxygen and nitrogen atoms of the adduct. This internal rearrangement transforms the initially carbamic acid (-NHCOOH) into a more thermally stable zwitterionic ($–NH_2^+COO^-$) adduct (**Figure S5**). The proton signal labelled as H8 exhibits a gradual downfield shift from 9.37 to

6.44 ppm over the heating period (15, 30 and 45 min, respectively). Further evidence comes from the observed shift of the carbamate carbon peak in the ^{13}C NMR spectrum, which experiences a downfield shift from 158.9 ppm to 161.3 ppm upon heating.[27]

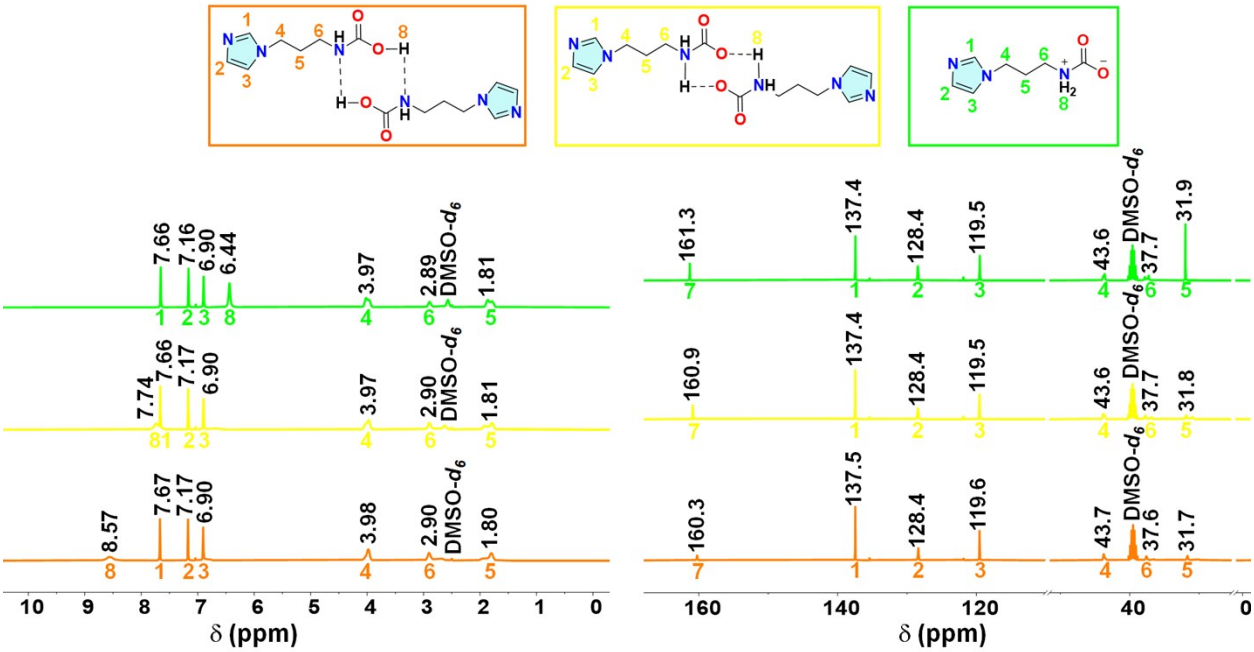

Figure S5. Stacked $^{1}H/^{13}C$ NMR spectra of the api-CO_2 adduct in DMSO-d_6, measured at 15, 30, and 40 min (orange, yellow, and green colors) after thermal heating at 80 °C.

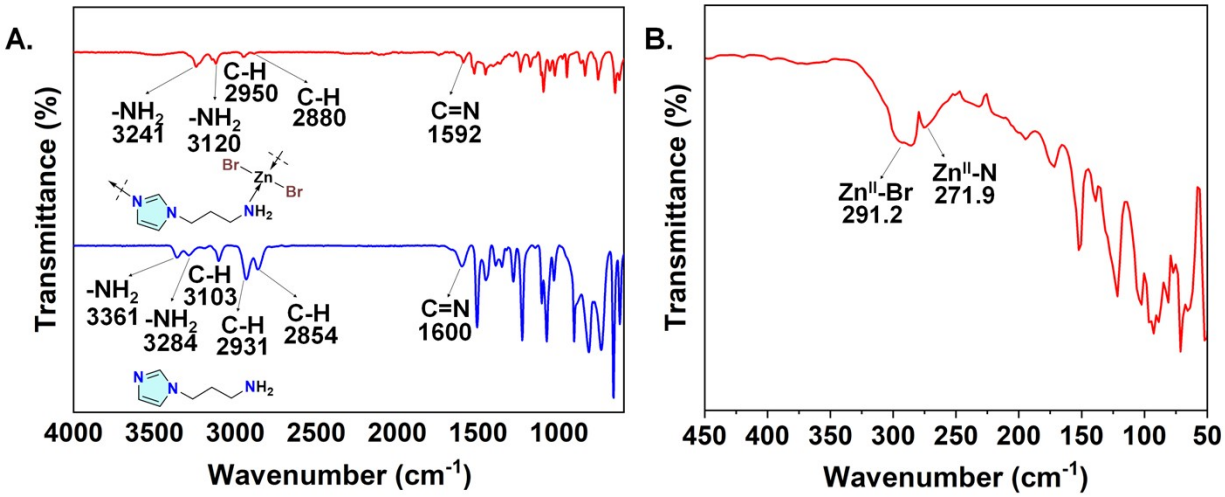

Figure S6. A. Mid-range ATR-FTIR spectra of api (blue trace) and the Zn-api complex (red trace). **B.** Far-range ATR-FTIR spectrum of the Zn-api complex. All spectra were recorded for solid samples, with the Zn-api complex prepared in DMSO.

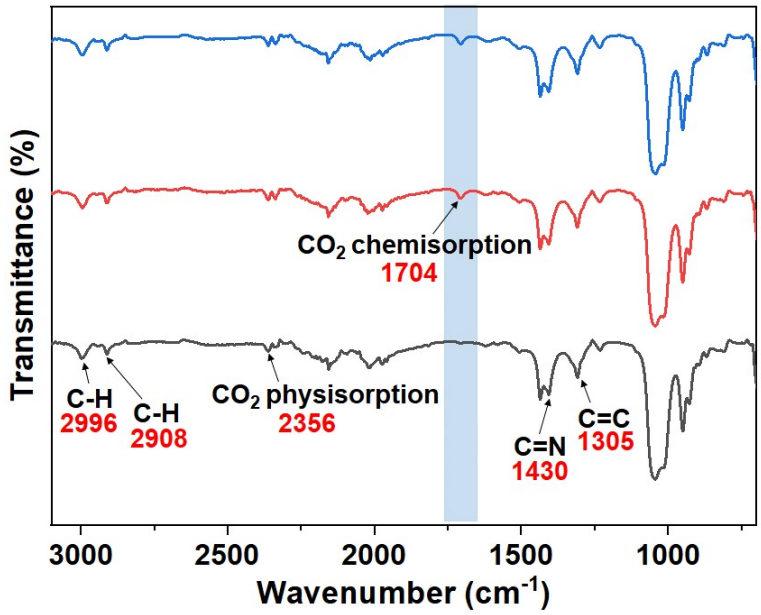

Figure S7. *In situ* ATR-FTIR spectra of the Zn-api complex in DMSO (black trace), measured after 30 min (red trace) and 6 h (blue trace) of exposure to a CO_2 balloon.

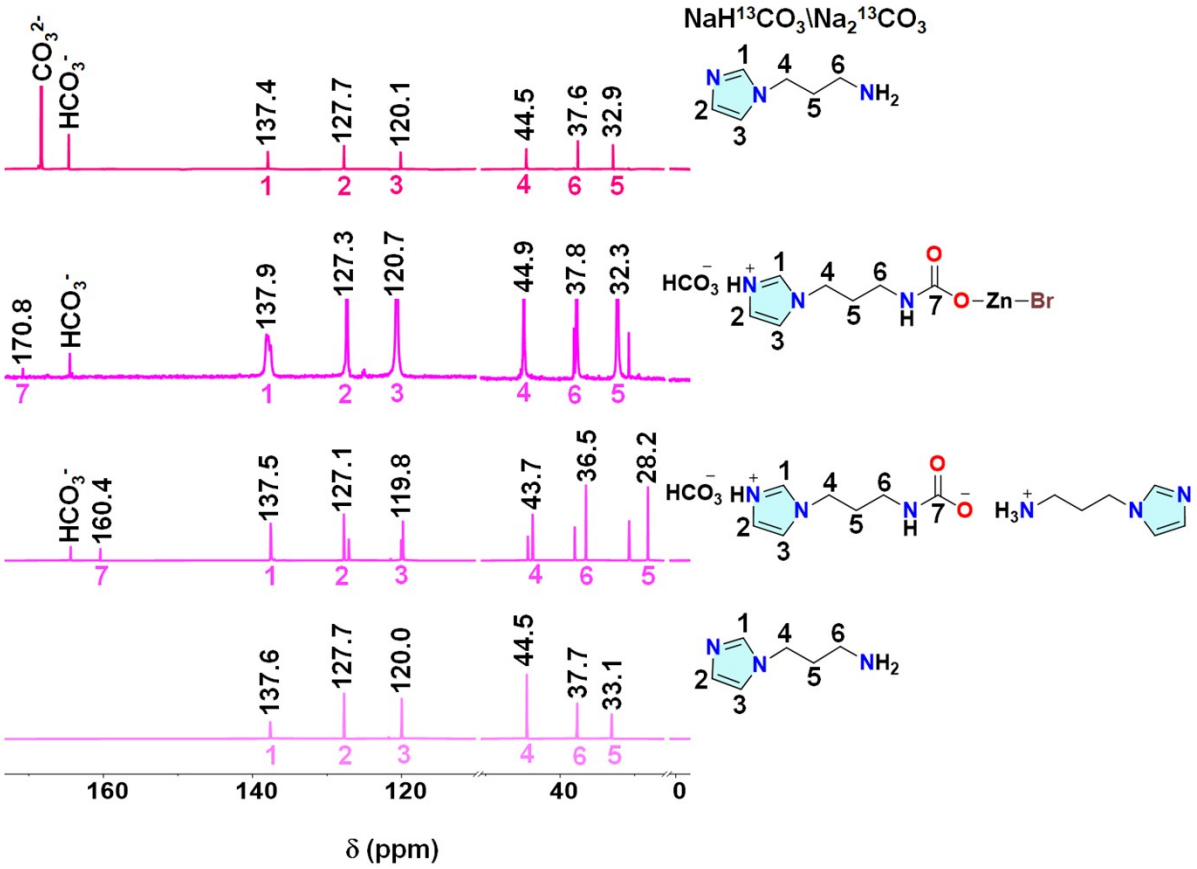

Figure S8. ^{13}C NMR spectra in D_2O for api, api-CO_2, Zn-api-CO_2 complex, $Na_2{}^{13}CO_3$/api

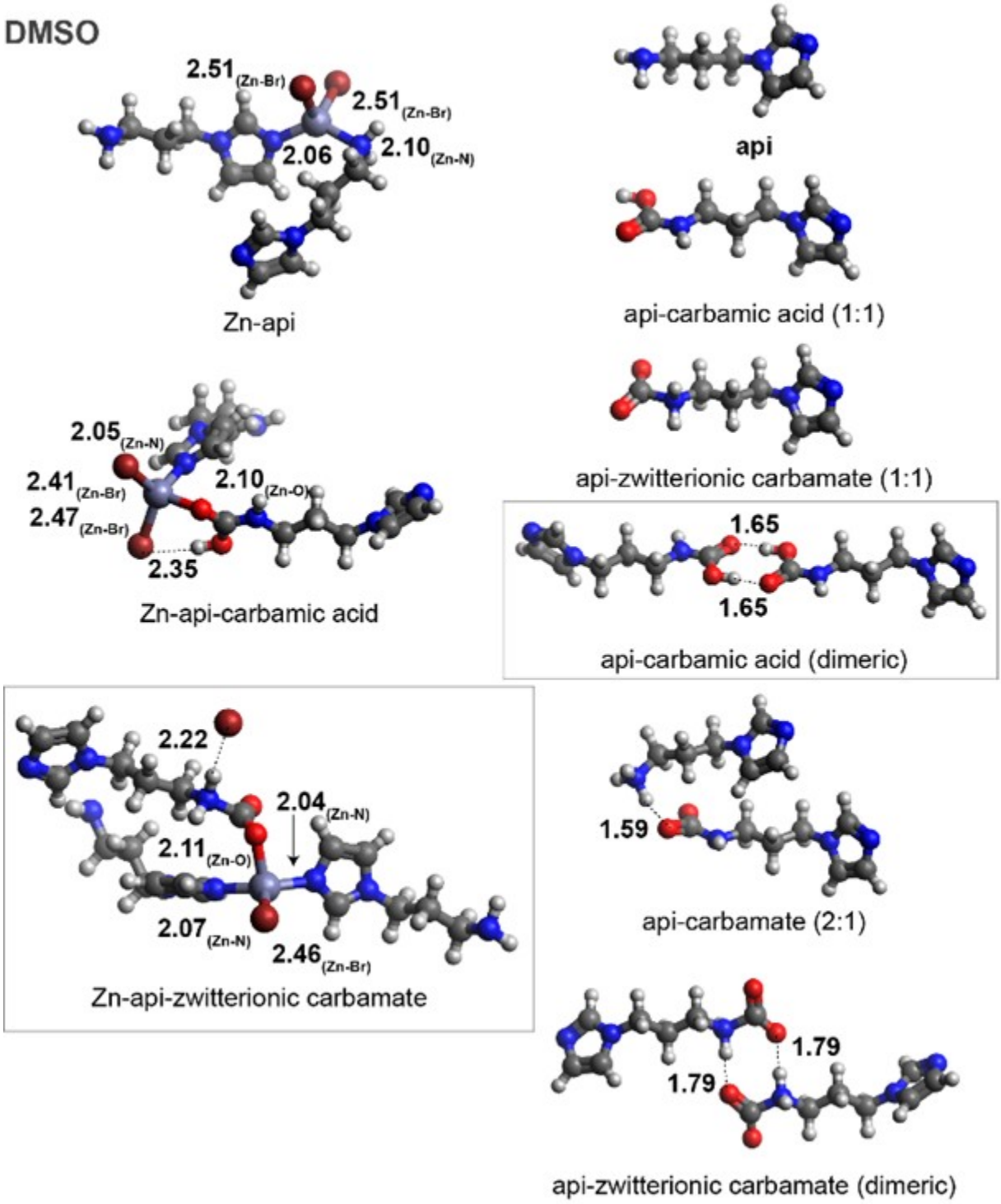

Figure S9. DFT optimized structures of the Zn-api complex and free api, along with their postulated CO_2 adducts in DMSO.

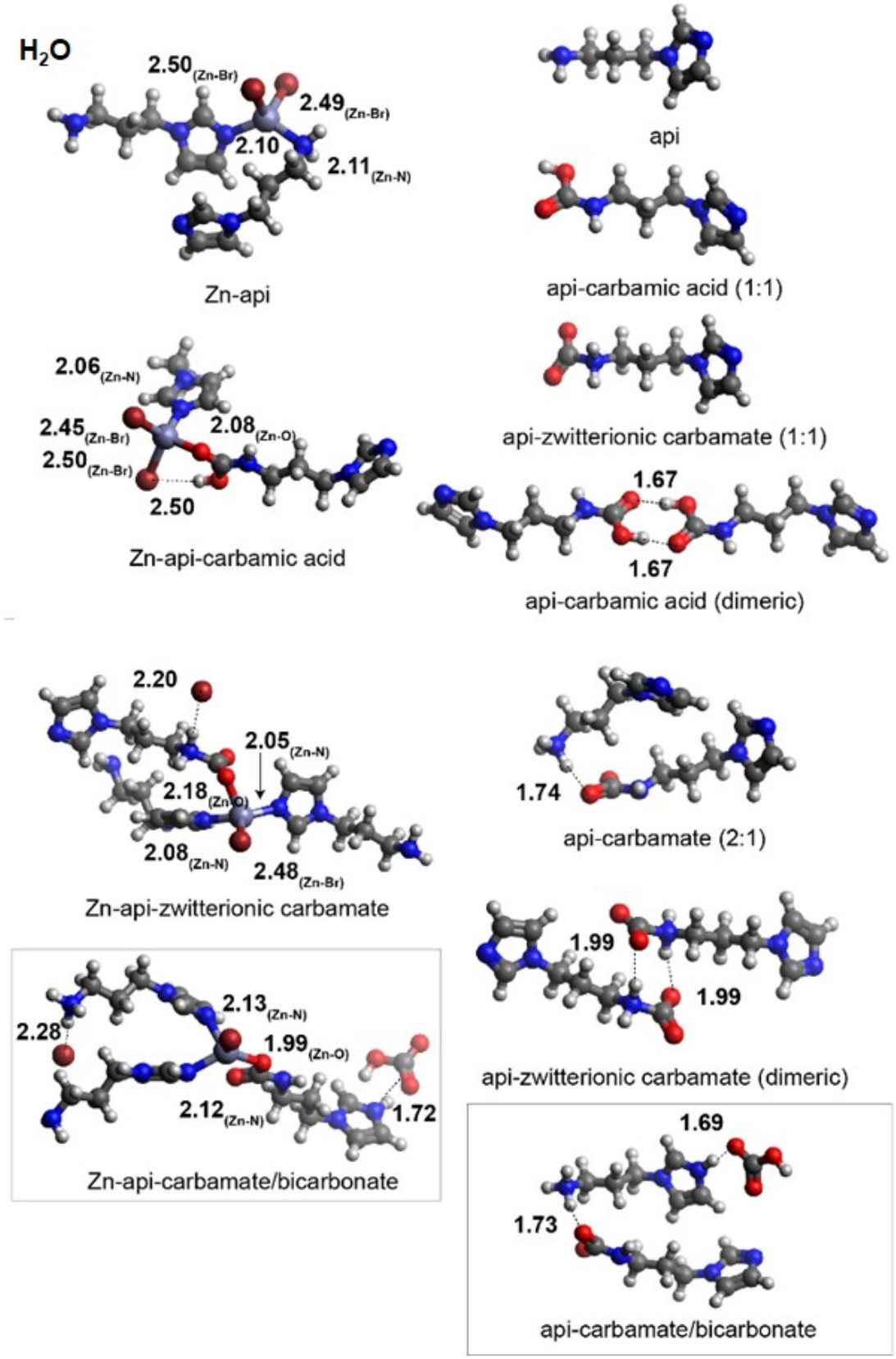

Figure S10. DFT optimized structures of the Zn-api complex and free api, along with their postulated CO_2 adducts in water.

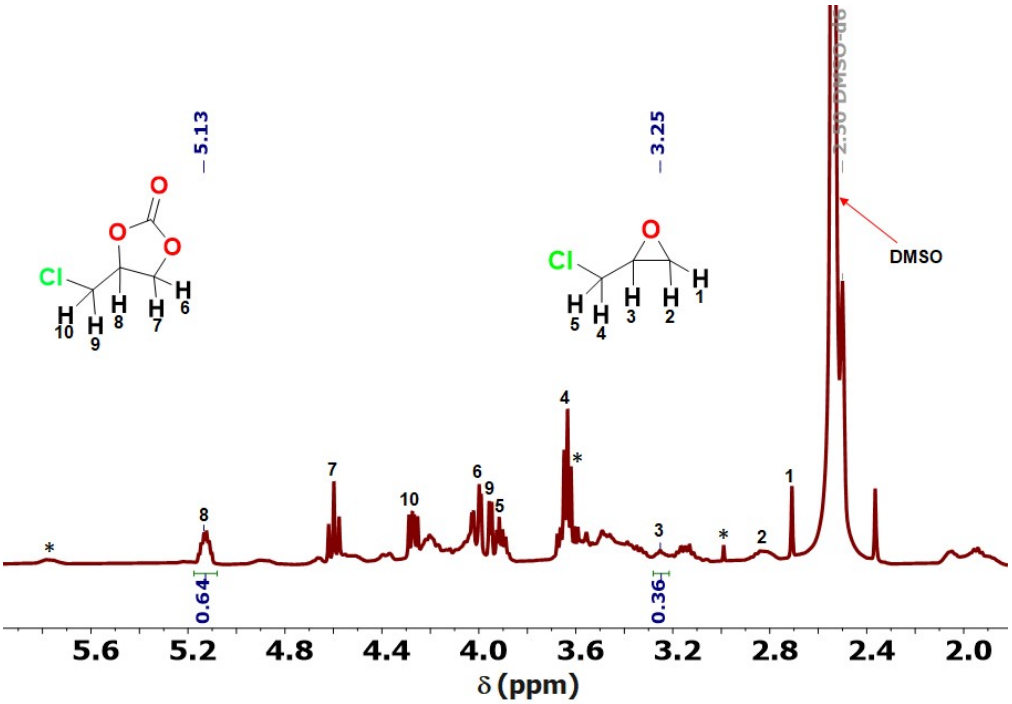

Figure S11. ^{1}H NMR spectrum (measured in DMSO-d_6) of the conversion of ECH into the 4-chloromethyl-2-oxo-1,3-dioxolane catalyzed by 15 mol% Zn-api in 0.5 mL DMSO at 1 atm CO_2 (balloon) and 80 ºC for 24 h (Entry 1, Table 2). *Catalyst peaks.

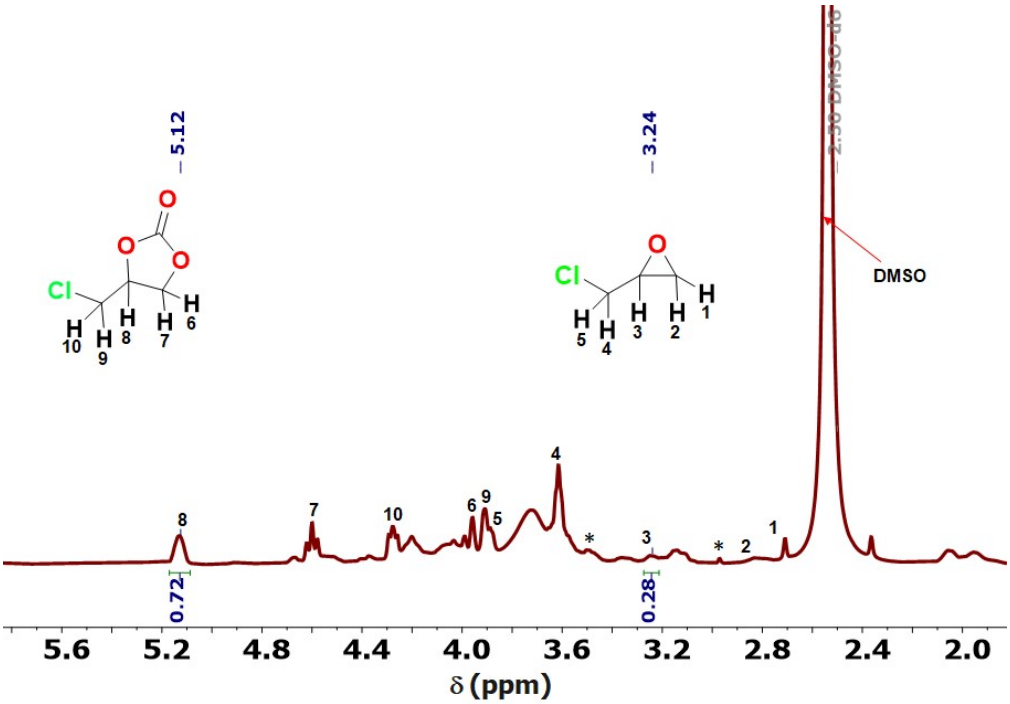

Figure S12. ^{1}H NMR spectrum (measured in DMSO-d_6) of the conversion of ECH into the 4-chloromethyl-2-oxo-1,3-dioxolane catalyzed by 10 mol% Zn-api in 0.5 mL DMSO at 1 atm CO_2 (balloon) and 80 ºC for 24 h (Entry 2, Table 2). *Catalyst peaks.

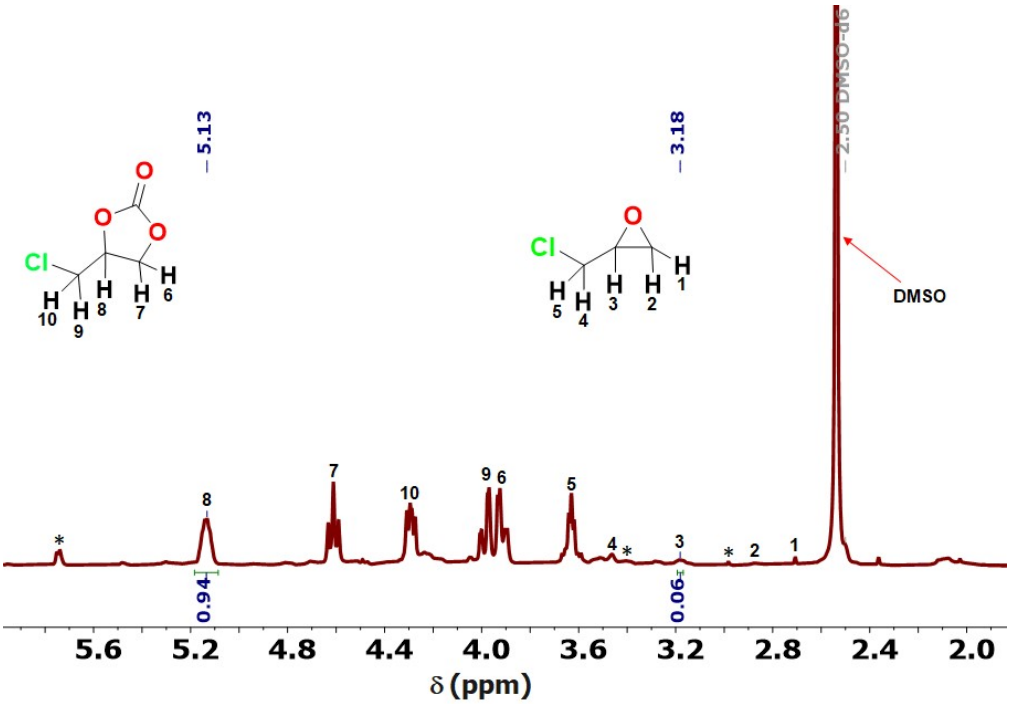

Figure S13. ^{1}H NMR spectrum (measured in DMSO-d_6) of the conversion of ECH into the 4-chloromethyl-2-oxo-1,3-dioxolane catalyzed by 5 mol% Zn-api in 0.5 mL DMSO at 1 atm CO_2 (balloon) and 80 ºC for 24 h (Entry 3, Table 2). *Catalyst peaks

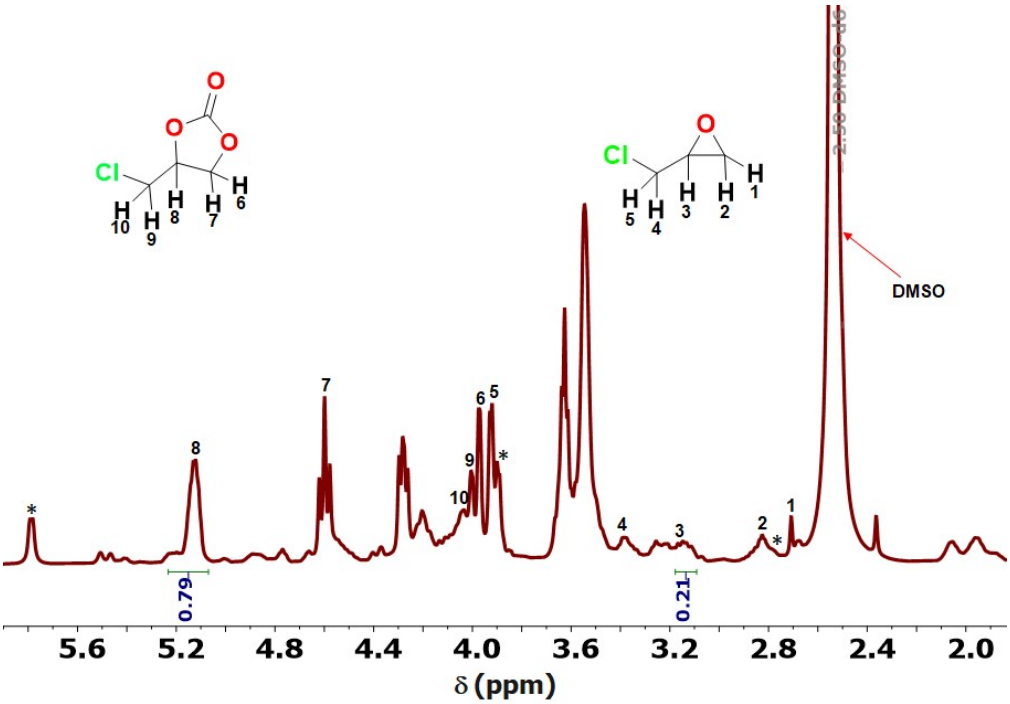

Figure S14. ^{1}H NMR spectrum (measured in DMSO-d_6) of the conversion of ECH into the 4-chloromethyl-2-oxo-1,3-dioxolane catalyzed by 5 mol% Zn-api in 0.5 mL DMSO at 1 atm CO_2 (balloon) and 40 ºC for 24 h (Entry 4, Table 2). *Catalyst peaks

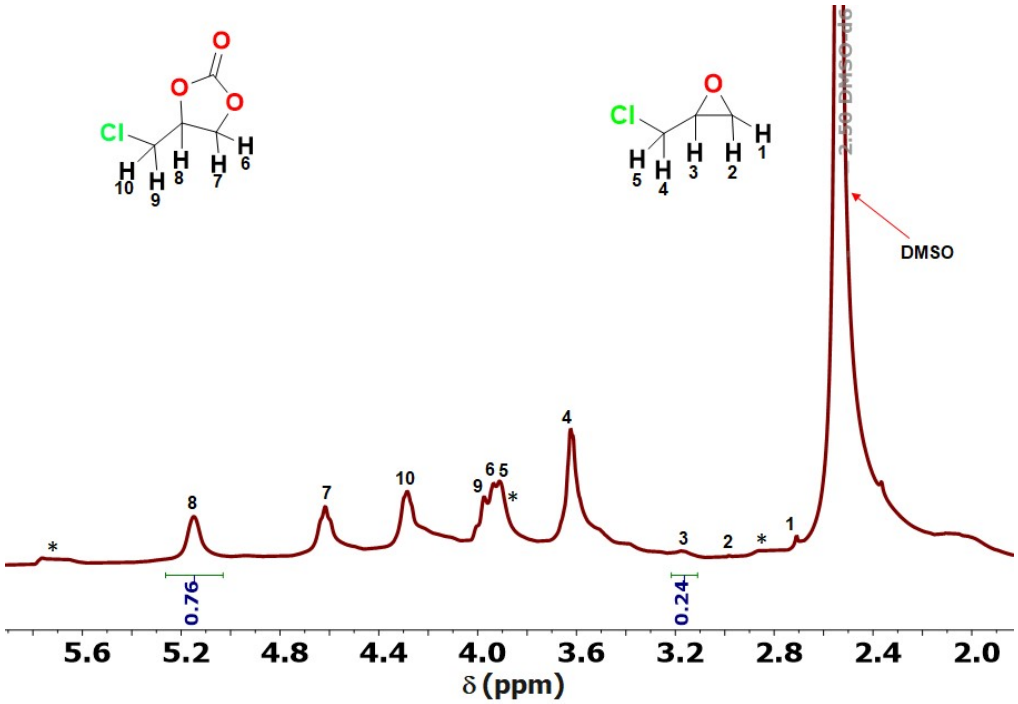

Figure S15. ^{1}H NMR spectrum (measured in DMSO-d_6) of the conversion of ECH into the 4-chloromethyl-2-oxo-1,3-dioxolane catalyzed by 5 mol% Zn-api in 0.5 mL DMSO at 1 atm CO_2 (balloon) and 80 ºC for 16 h (Entry 5, Table 2). *Catalyst peaks

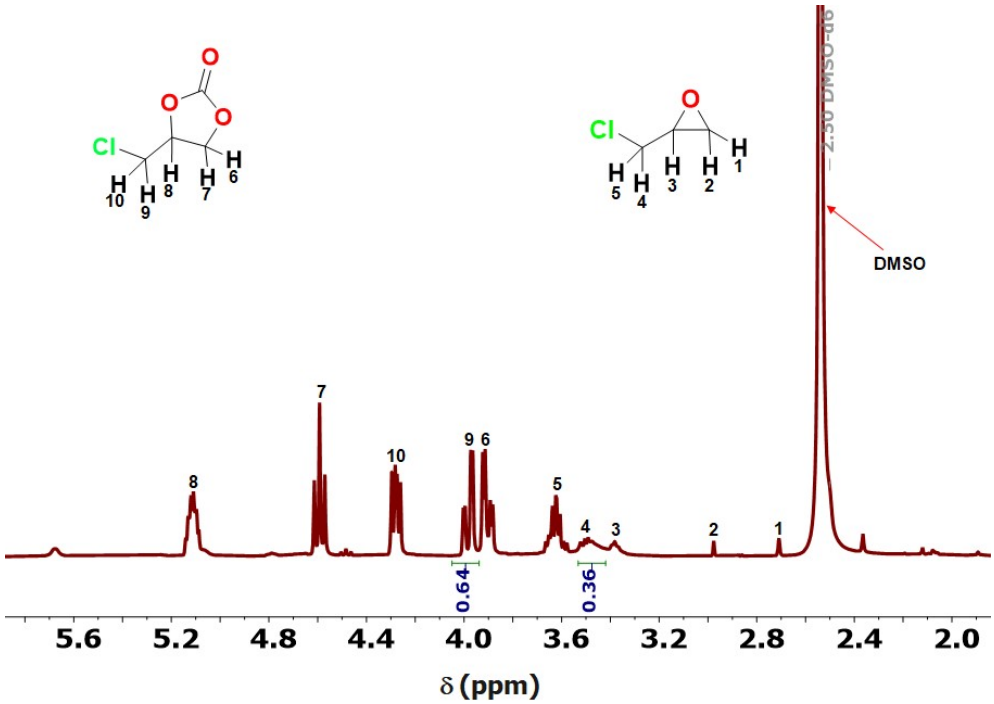

Figure S16. ^{1}H NMR spectrum (measured in DMSO-d_6) of the conversion of ECH into the 4-chloromethyl-2-oxo-1,3-dioxolane catalyzed by 5 mol% $ZnBr_2$ in 0.5 mL DMSO at 1 atm CO_2 (balloon) and 80 ºC for 24 h (Entry 6, Table 2).

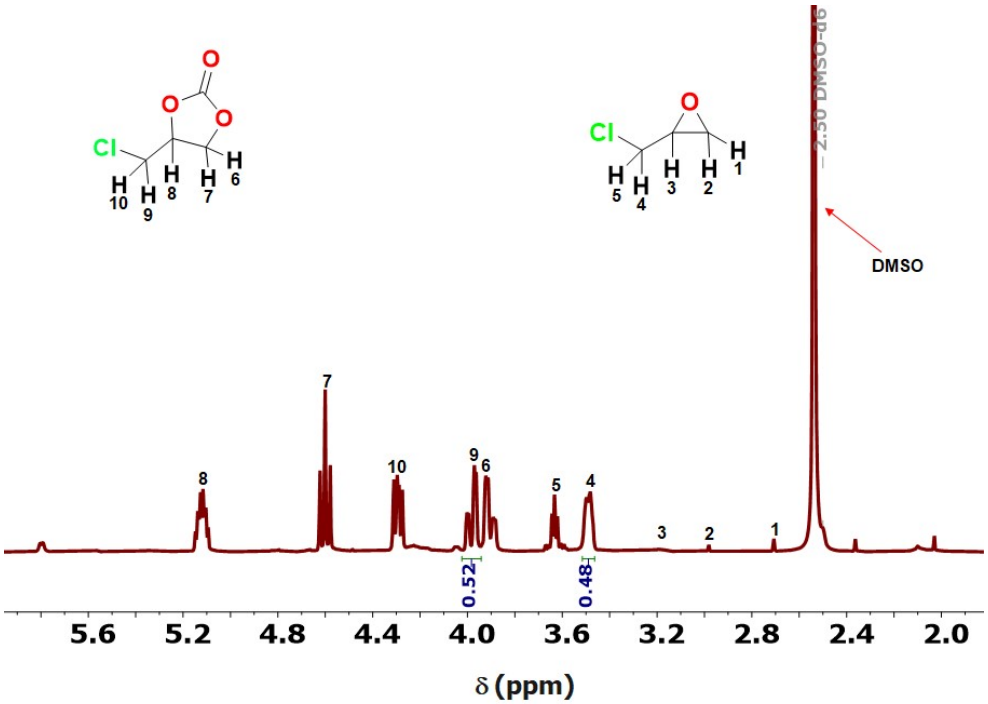

Figure S17. ^{1}H NMR spectrum (measured in DMSO-d_6) of the conversion of ECH into the 4-chloromethyl-2-oxo-1,3-dioxolane catalyzed by 5 mol% api in 0.5 mL DMSO at 1 atm CO_2 (balloon) and 80 ºC for 24 h (Entry 7, Table 2).

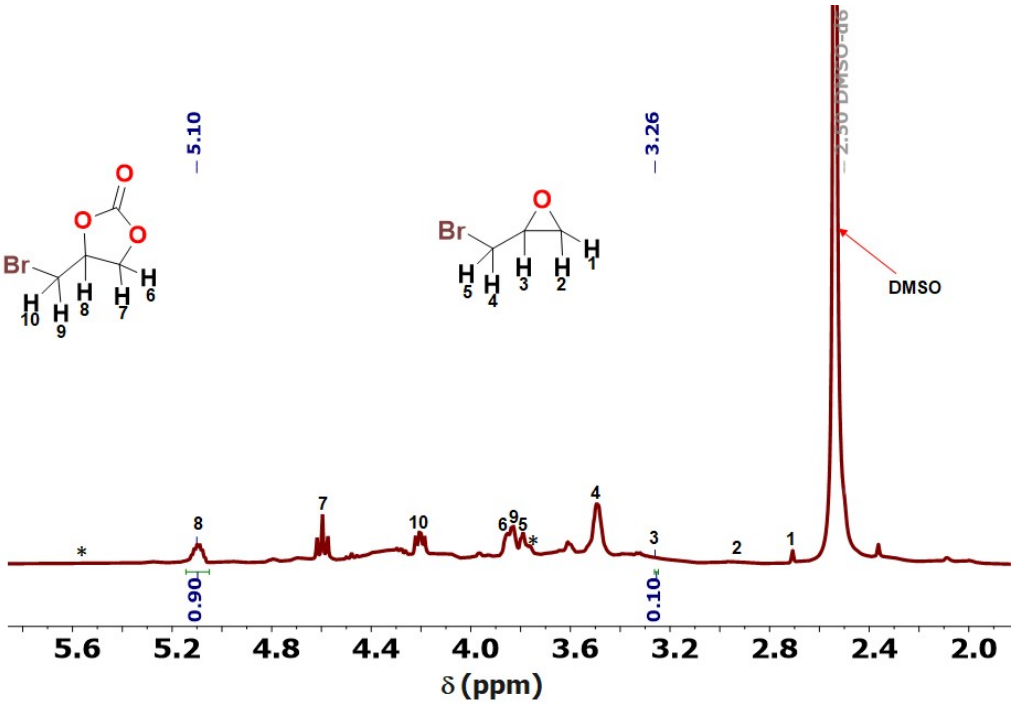

Figure S18. ^{1}H NMR spectrum (measured in DMSO-d_6) of the conversion of EBH into the 4-bromomethyl-2-oxo-1,3-dioxolane catalyzed by 5 mol% Zn-api in 0.5 mL DMSO at 1 atm CO_2 (balloon) and 80 ºC for 24 h (Entry 2, Table 3). *Catalyst peaks

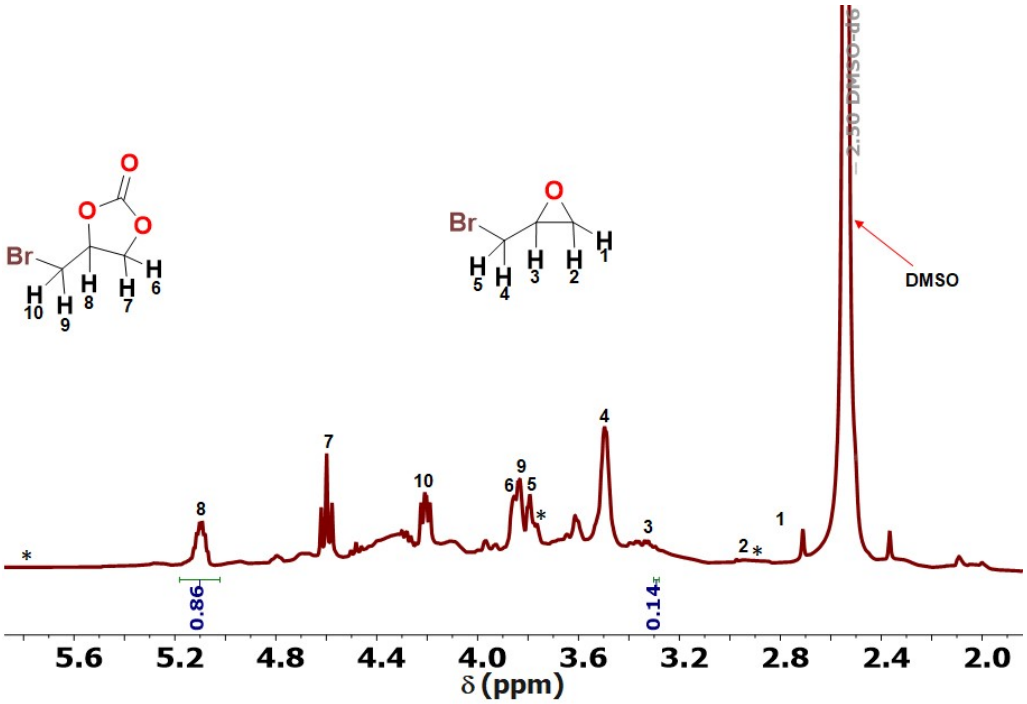

Figure S19. ^{1}H NMR spectrum (measured in DMSO-d_6) of the conversion of EBH into the 4-bromomethyl-2-oxo-1,3-dioxolane catalyzed by 15 mol% Zn-api in 0.5 mL DMSO at 1 atm CO_2 (balloon) and 80 ºC for 24 h (Footnote, Table 3). *Catalyst peaks.

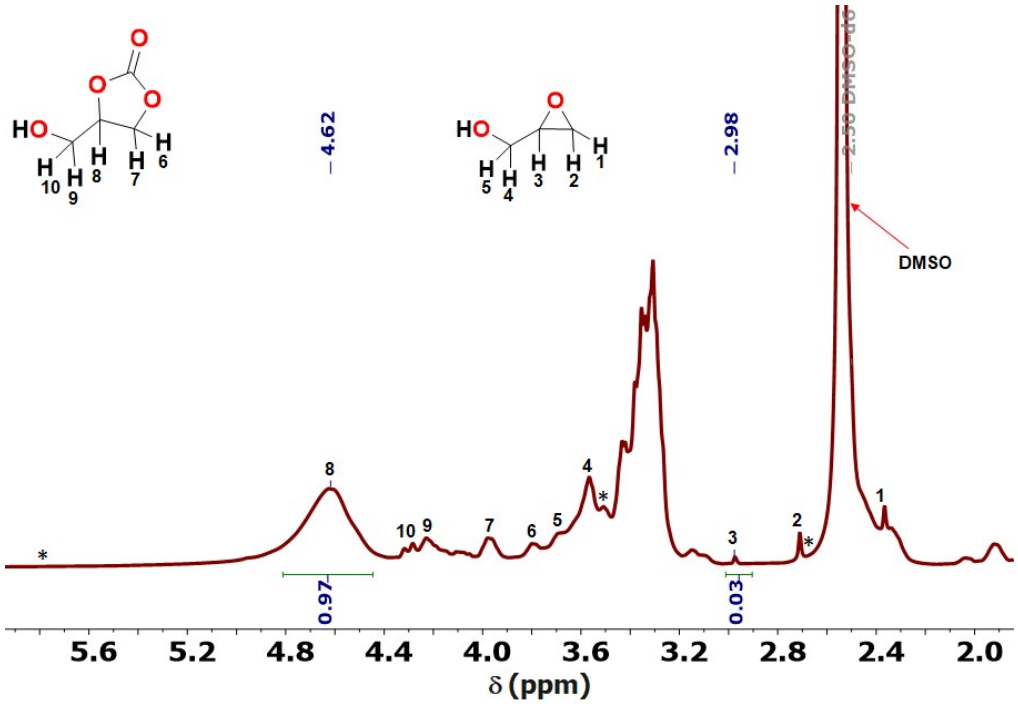

Figure S20. ^{1}H NMR spectrum (measured in DMSO-d_6) of the conversion of GO into the 4-(hydroxymethyl)-1,3-dioxolan-2-one catalyzed by 5 mol% Zn-api in 0.5 mL DMSO at 1 atm CO_2 (balloon) and 80 ºC for 24 h (Entry 3, Table 3). *Catalyst peaks.

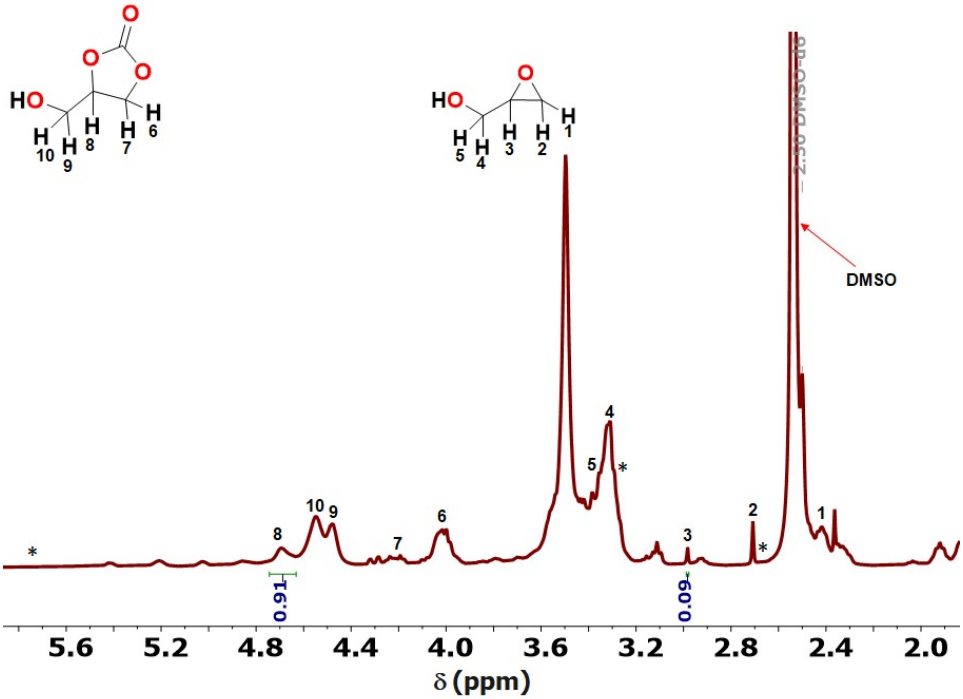

Figure S21. ^{1}H NMR spectrum (measured in DMSO-d_6) of the conversion of GO into the 4-(hydroxymethyl)-1,3-dioxolan-2-one catalyzed by 15 mol% Zn-api in 0.5 mL DMSO at 1 atm CO_2 (balloon) and 80 ºC for 24 h (Footnote, Table 3). *Catalyst peaks.

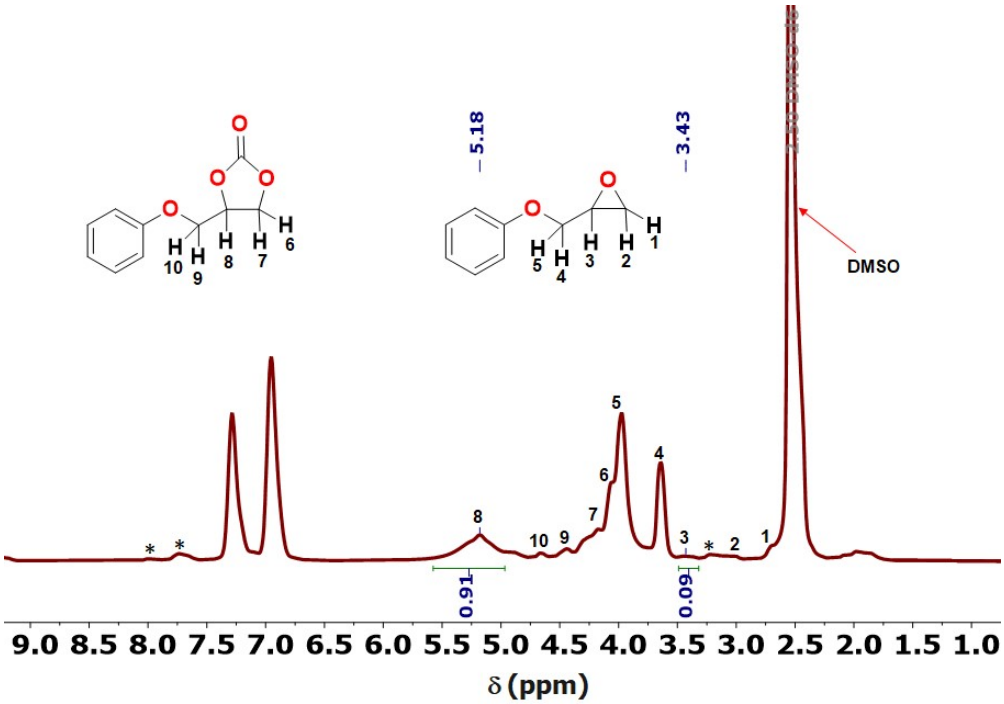

Figure S22. ^{1}H NMR spectrum (measured in DMSO-d_6) of the conversion of POP into the 4-(phenoxymethyl)-1,3-dioxolan-2-one catalyzed by 5 mol% Zn-api in 0.5 mL DMSO at 1 atm CO_2 (balloon) and 80 ºC for 24 h (Entry 4, Table 3). *Catalyst peaks.

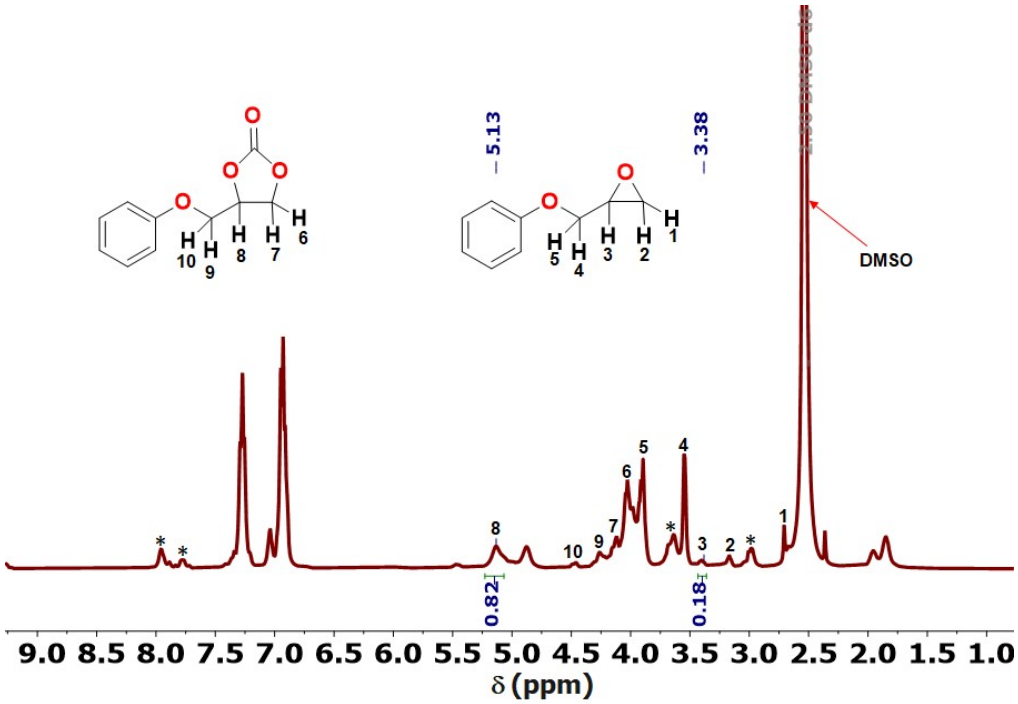

Figure S23. ^{1}H NMR spectrum (measured in DMSO-d_6) of the conversion of POP into the 4-(phenoxymethyl)-1,3-dioxolan-2-one catalyzed by 15 mol% Zn-api in 0.5 mL DMSO at 1 atm CO_2 (balloon) and 80 ºC for 24 h (Footnote, Table 3). *Catalyst peaks.

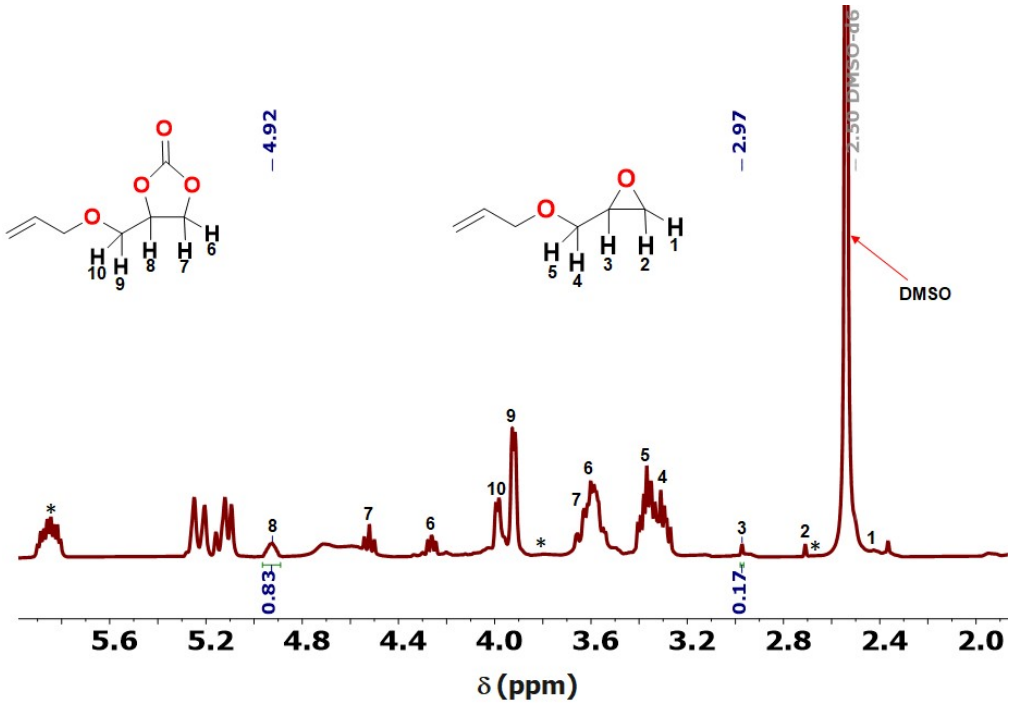

Figure S24. ^{1}H NMR spectrum (measured in DMSO-d_6) of the conversion of AEG into 4-((allyloxy)methyl)-1,3-dioxolan-2-one catalyzed by 5 mol% Zn-api in 0.5 mL DMSO at 1 atm CO_2 (balloon) and 80 ºC for 24 h (Table 3, Entry 5). *Catalyst peaks.

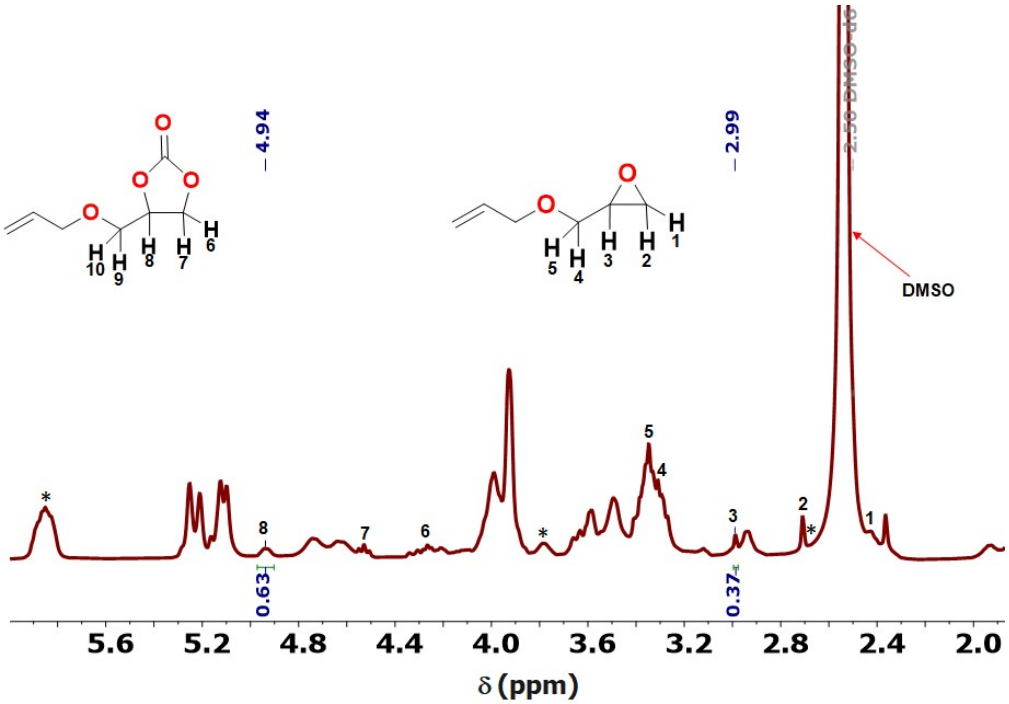

Figure S25. ^{1}H NMR spectrum (measured in DMSO-d_6) of the conversion of AEG into the 4-((allyloxy)methyl)-1,3-dioxolan-2-one catalyzed by 15 mol% Zn-api in 0.5 mL DMSO at 1 atm CO_2 (balloon) and 80 ºC for 24 h (Footnote, Table 3). *Catalyst peaks.

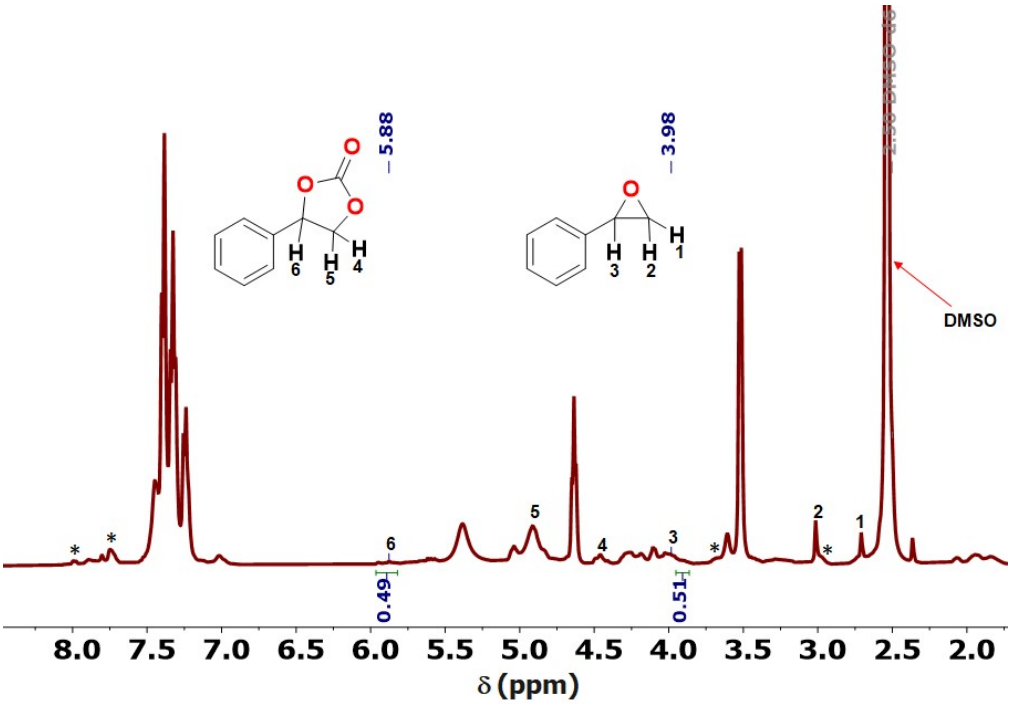

Figure S26. ^{1}H NMR spectrum (measured in DMSO-d_6) of the conversion of SO into the 4-phenyl-1,3-dioxolan-2-one catalyzed by 5 mol% Zn-api in 0.5 mL DMSO at 1 atm CO_2 (balloon) and 80 ºC for 24 h (Entry 6, Table 3). *Catalyst peaks.

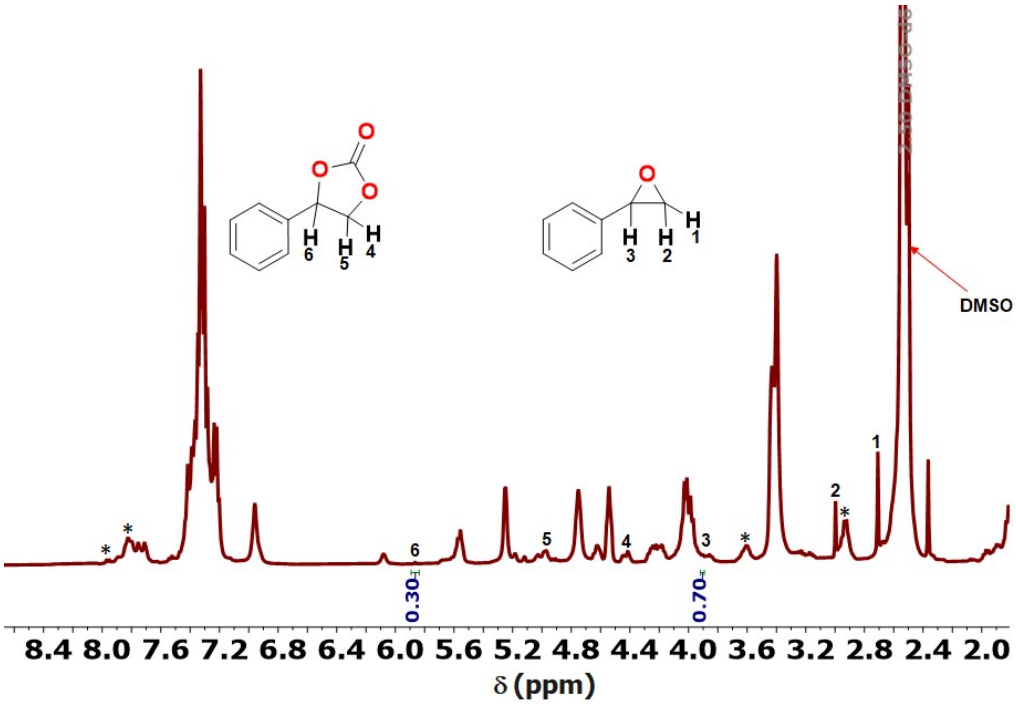

Figure S27. ^{1}H NMR spectrum (measured in DMSO-d_6) of the conversion of SO into the 4-phenyl-1,3-dioxolan-2-one catalyzed by 15 mol% Zn-api in 0.5 mL DMSO at 1 atm CO_2 (balloon) and 80 ºC for 24 h (Footnote, Table 3). *Catalyst peaks.

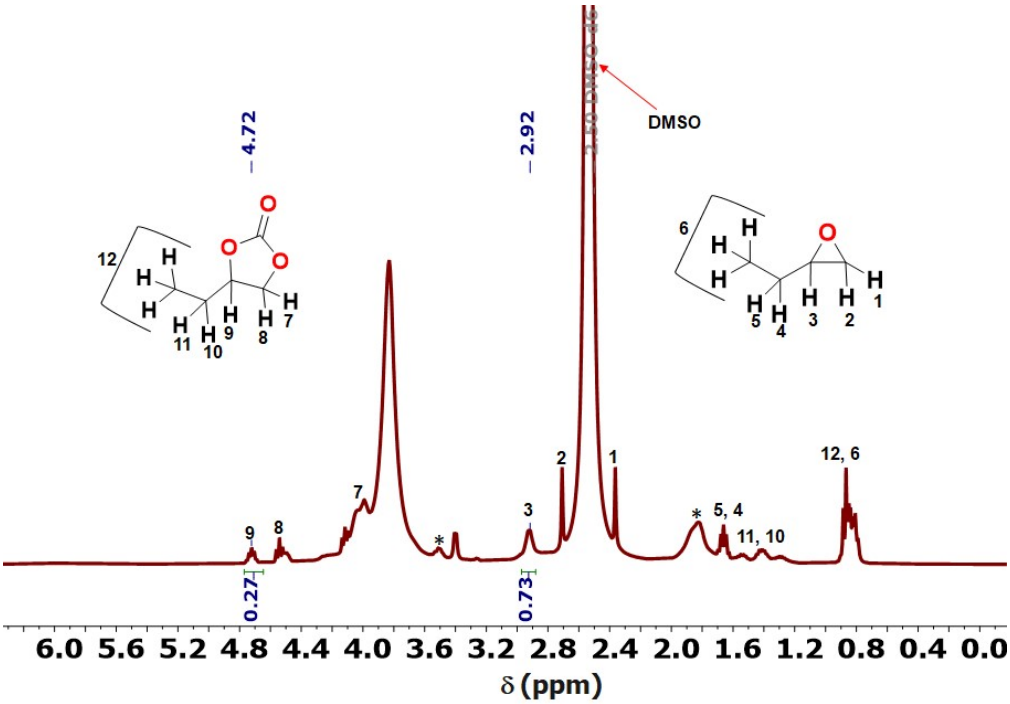

Figure S28. ^{1}H NMR spectrum (measured in DMSO-d_6) of the conversion of BO into the 4-ethyl-1,3-dioxolan-2-one catalyzed by 5 mol% Zn-api in 0.5 mL DMSO at 1 atm CO_2 (balloon) and RT for 24 h (Entry 7, Table 3). *Catalyst peaks.

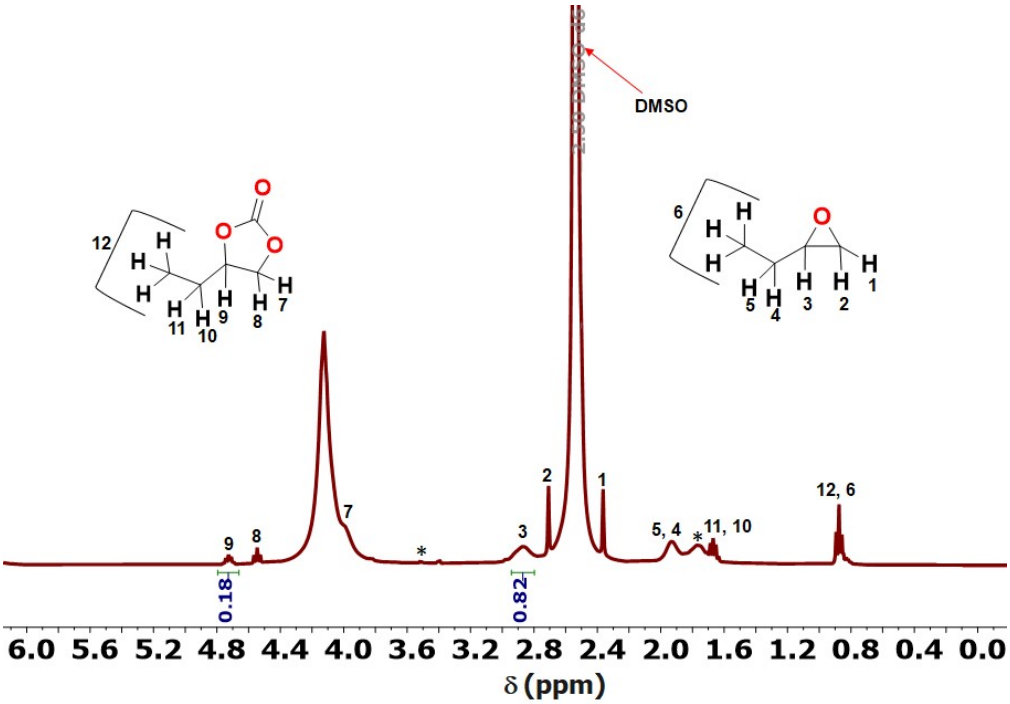

Figure S29. ^{1}H NMR spectrum (measured in DMSO-d_6) of the conversion of BO into the 4-ethyl-1,3-dioxolan-2-one catalyzed by 15 mol% Zn-api in 0.5 mL DMSO at 1 atm CO_2 (balloon) and RT for 24 h (Footnote, Table 3). *Catalyst peaks.

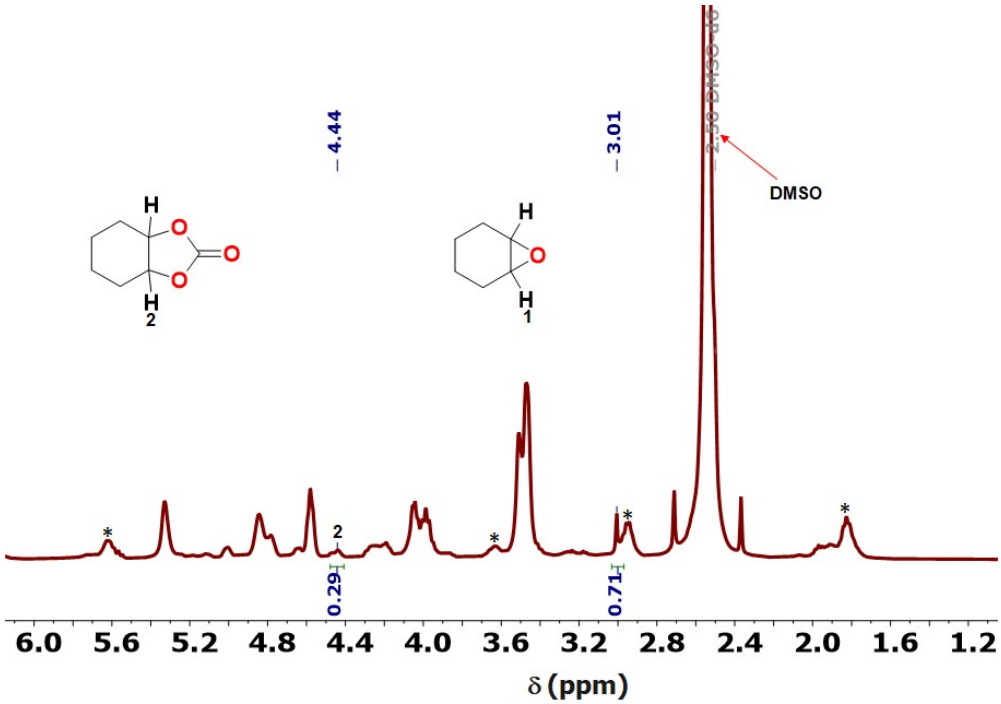

Figure S30. ^{1}H NMR spectrum (measured in DMSO-d_6) of the conversion of CHO into the hexahydrobenzo[d][1,3]dioxol-2-one catalyzed by 5 mol% Zn-api in 0.5 mL DMSO at 1 atm CO_2 (balloon) and 80 ºC for 24 h (Entry 8, Table 3). *Catalyst peaks.

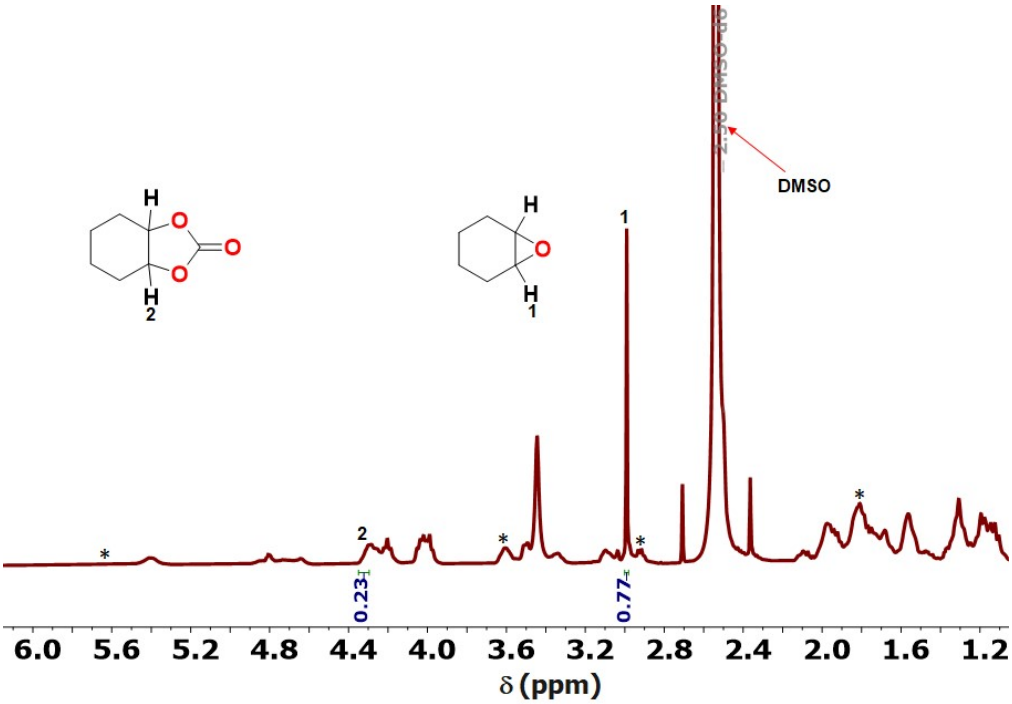

Figure S31. ^{1}H NMR spectrum (measured in DMSO-d_6) of the conversion of CHO into the hexahydrobenzo[d][1,3]dioxol-2-one catalyzed by 15 mol% Zn-api in 0.5 mL DMSO at 1 atm CO_2 (balloon) and 80 ºC for 24 h (Footnote, Table 3). *Catalyst peaks.

2. Isolation of CCs

The isolation of CCs was carried out in two stages. The first step involved separating the catalyst from the solution by adding 20 mL of chloroform to the reaction mixture, followed by filtration to remove the catalyst. In the second step, the filtrate was passed through a silica gel column, after which the chloroform was evaporated, and the CC was analyzed using ^{1}H/^{13}C NMR spectroscopy in DMSO- as shown in **Figures S31-S38**.

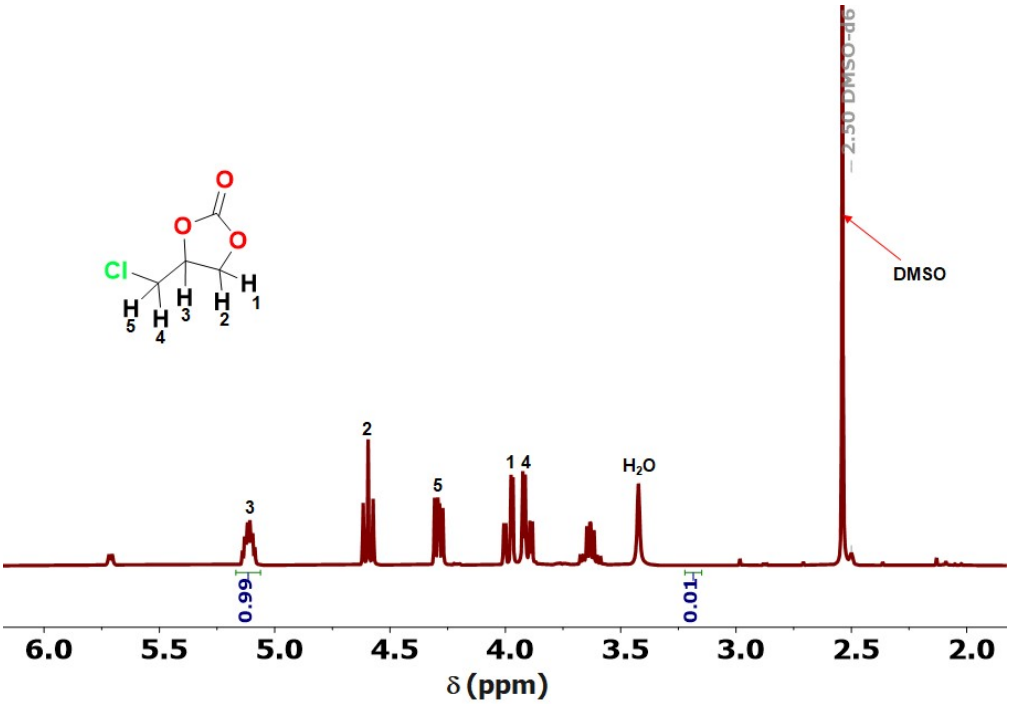

Figure S32. ^{1}H NMR spectrum of the isolated 4-chloromethyl-2-oxo-1,3-dioxolane. Yield: 92%.

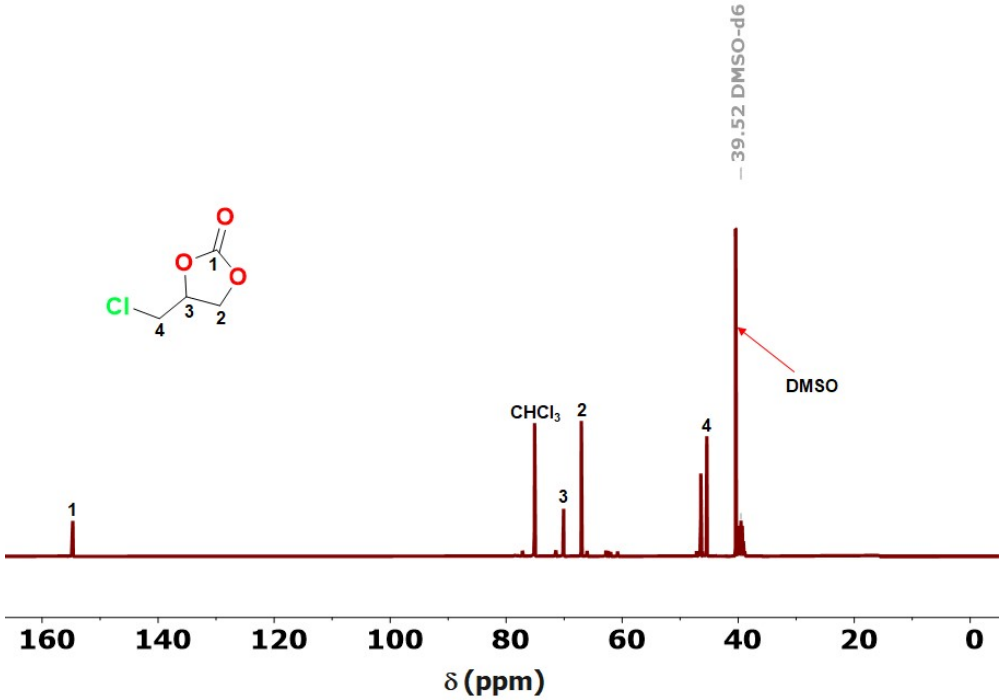

Figure S33. ^{13}C NMR spectrum of the isolated 4-chloromethyl-2-oxo-1,3-dioxolane.

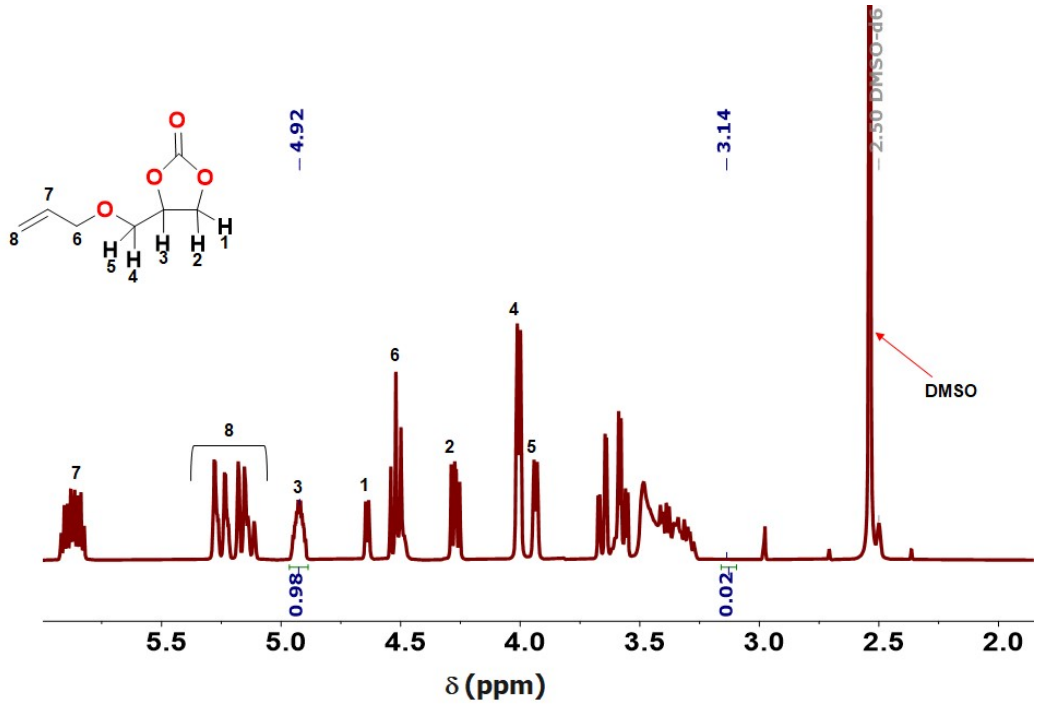

Figure S34. ^{1}H NMR spectrum of the isolated 4-((allyloxy)methyl)-1,3-dioxolan-2-one. Yield: 79%.

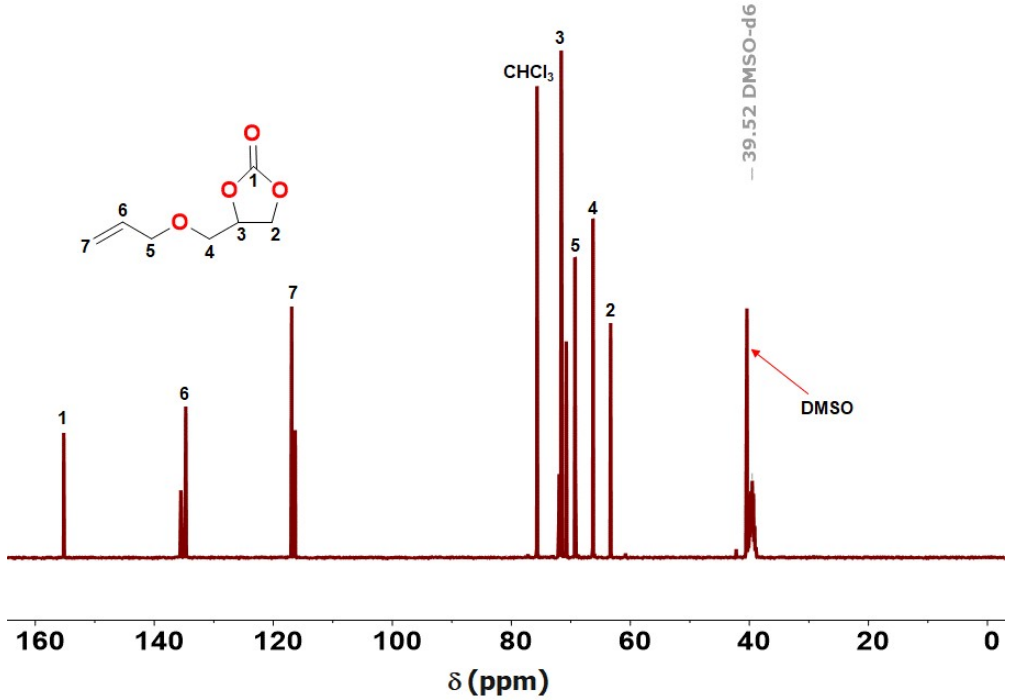

Figure S35. ^{13}C NMR spectrum of the isolated 4-((allyloxy)methyl)-1,3-dioxolan-2-one.

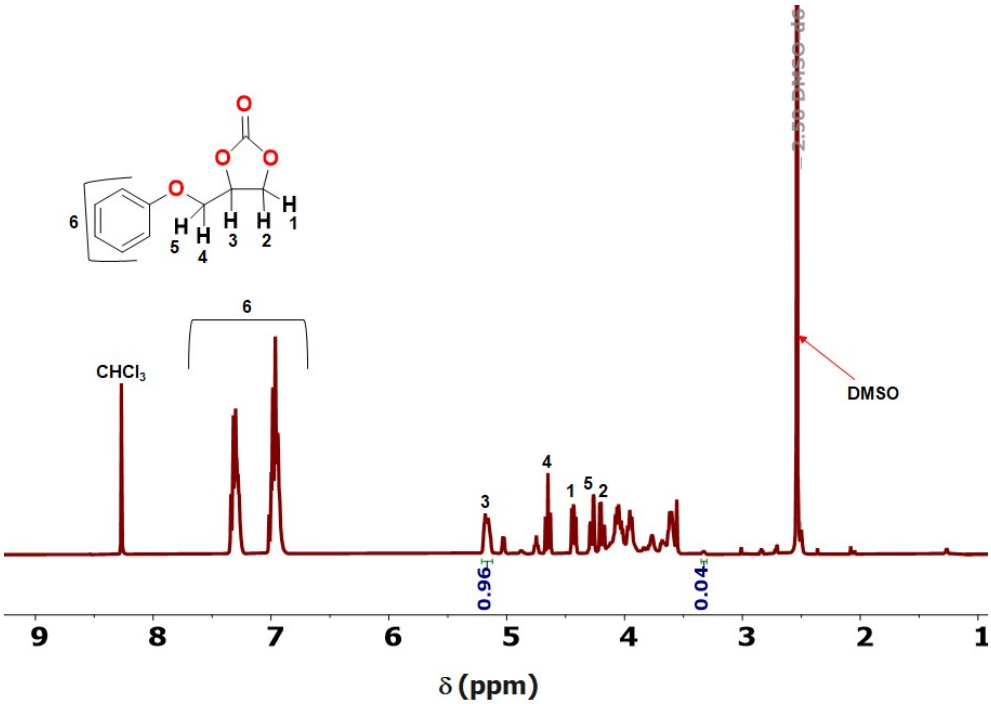

Figure S36. ^{1}H NMR spectrum of the isolated 4-(phenoxymethyl)-1,3-dioxolan-2-one. Yield: 81%.

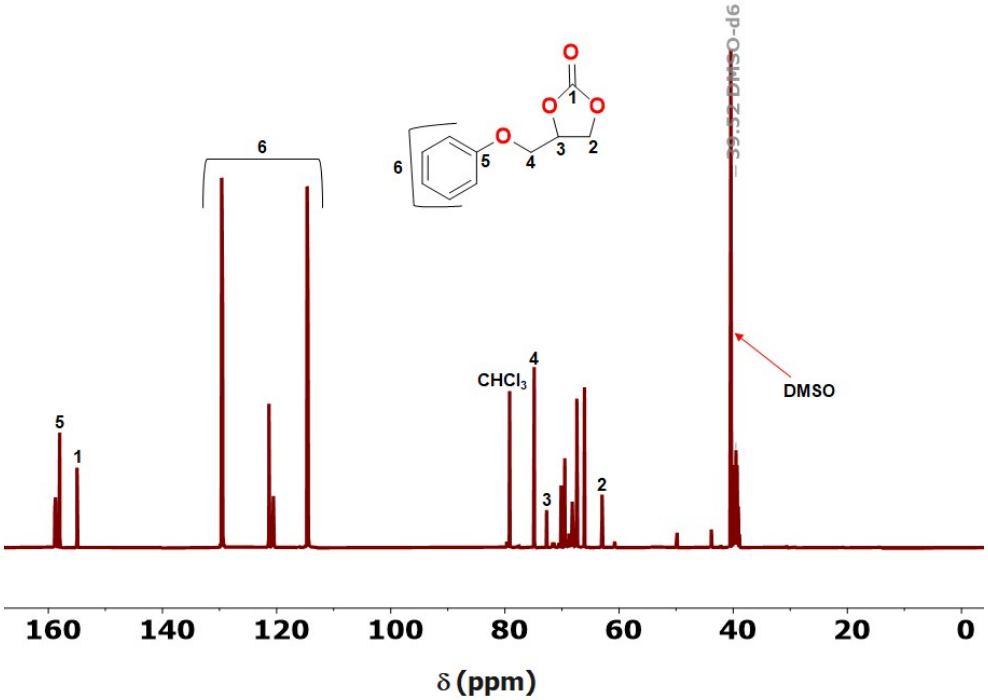

Figure S37. ^{13}C NMR spectrum of the isolated 4-(phenoxymethyl)-1,3-dioxolan-2-one.

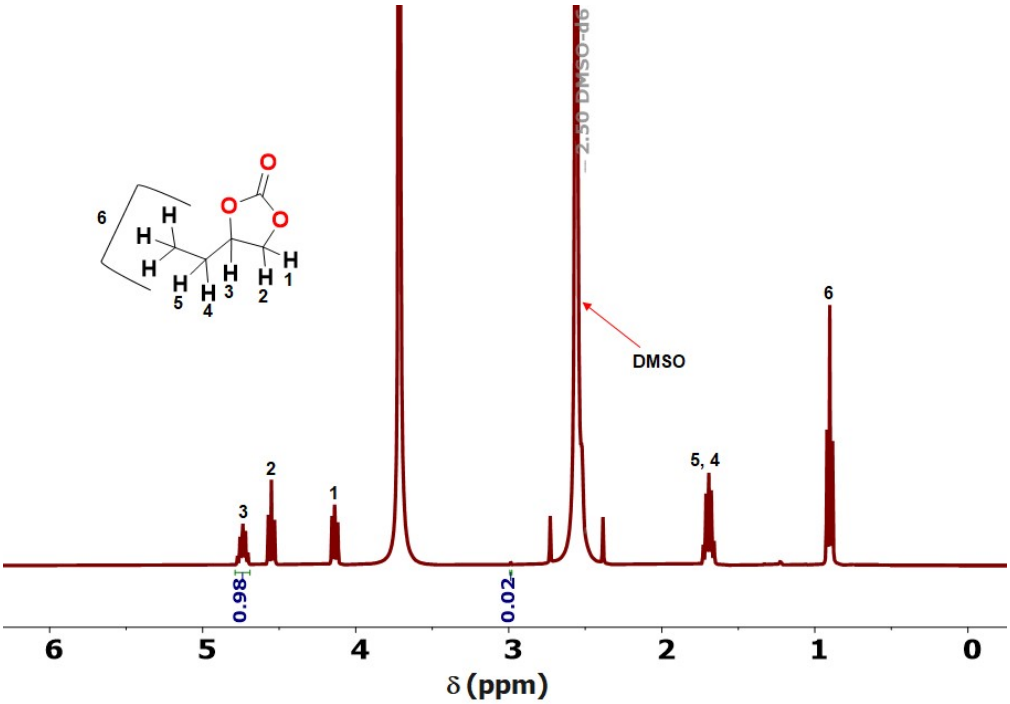

Figure S38. ^{1}H NMR spectrum of the isolated 4-ethyl-1,3-dioxolan-2-one. Yield: 22%.

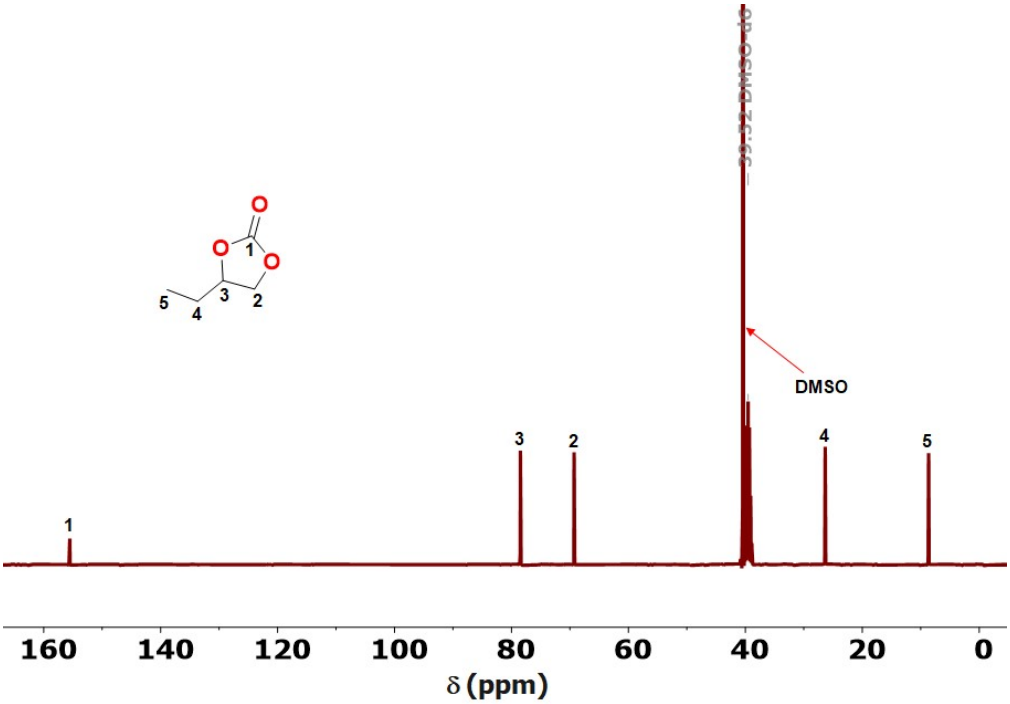

Figure S39. ^{13}C NMR spectrum of the isolated 4-ethyl-1,3-dioxolan-2-one.

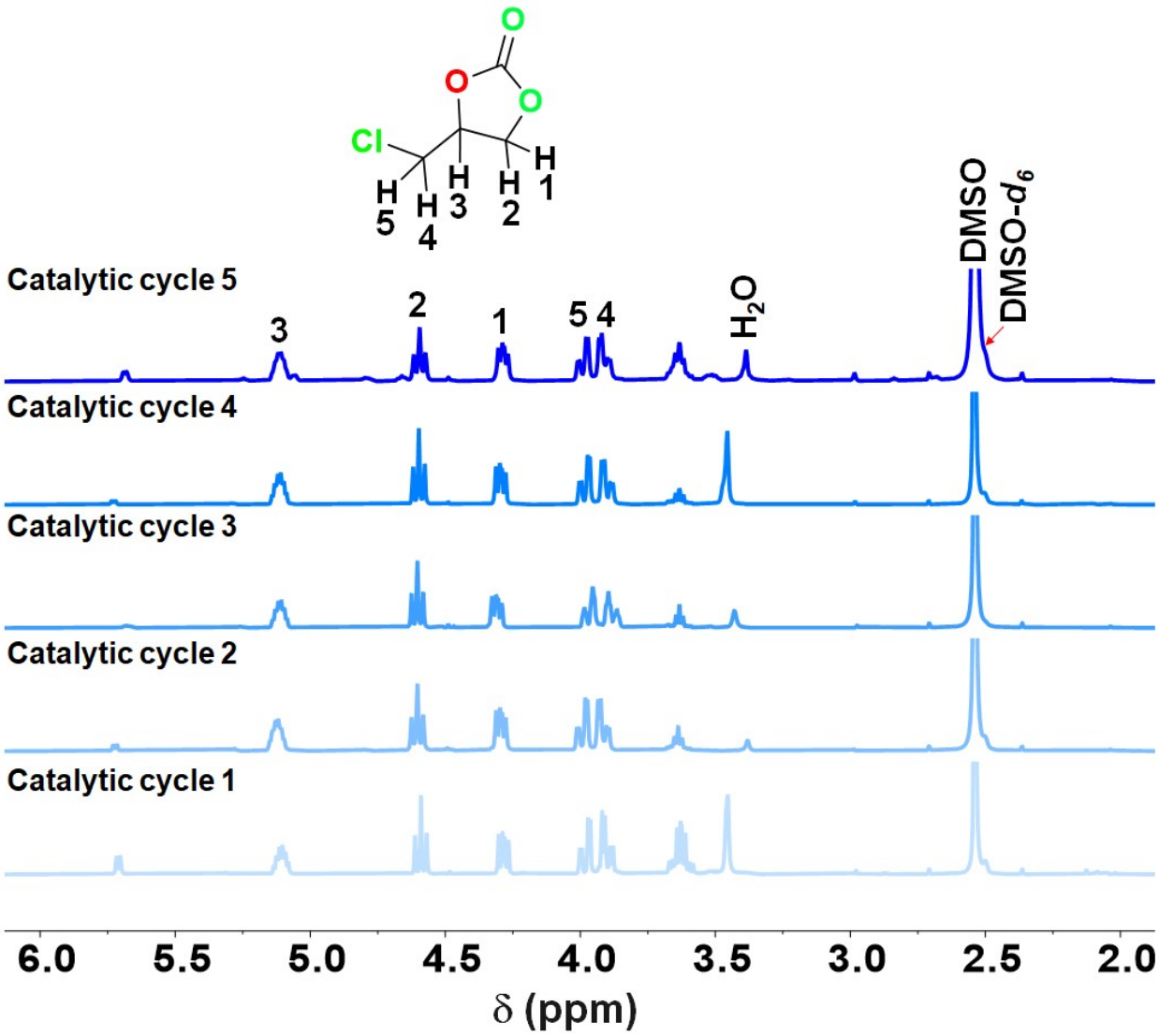

Figure S40. ^{1}H NMR spectra of the synthesized 4-chloromethyl-2-oxo-1,3-dioxolane over five catalytic cycles.

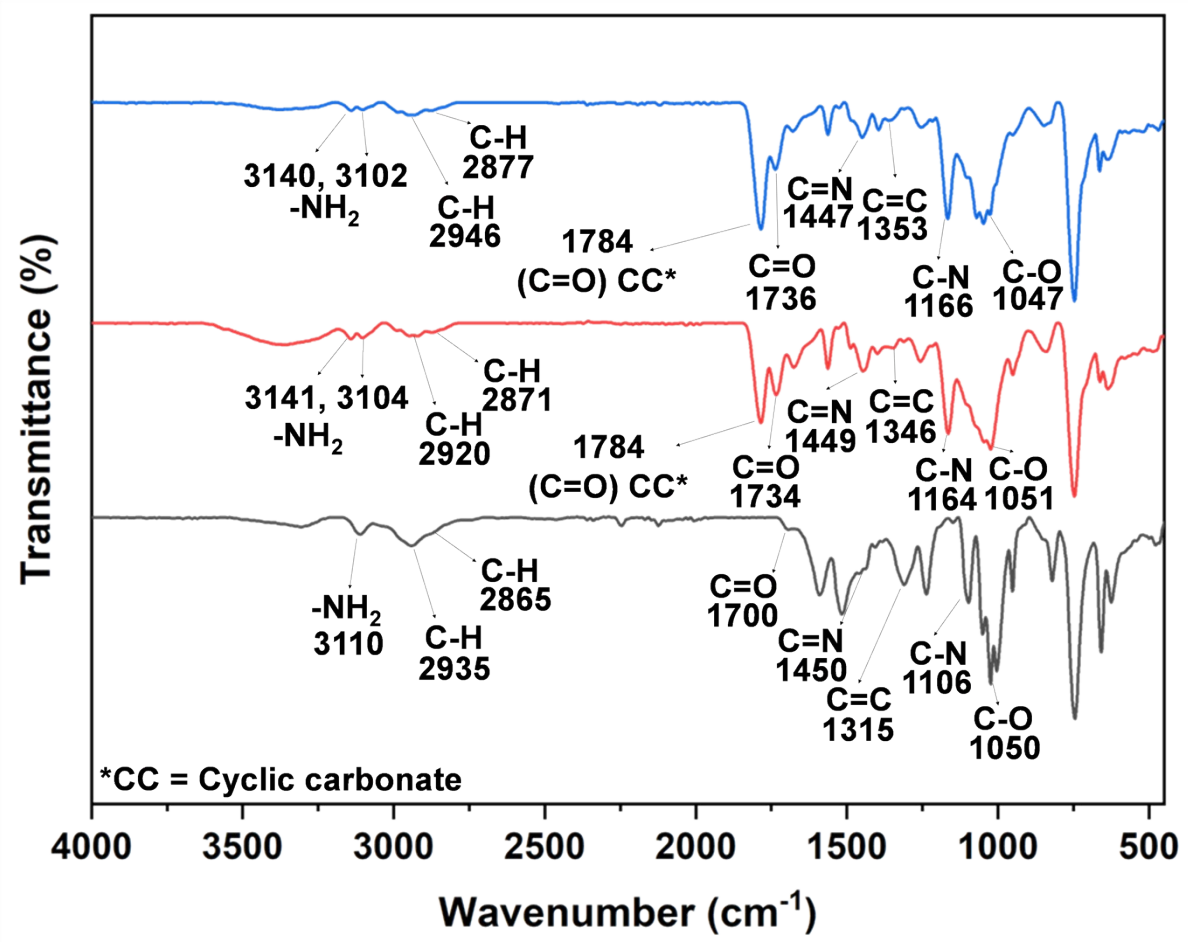

Figure S41. *Ex situ* ATR-FTIR spectra of the solid Zn-api-carbamate complex. Separate analyses were conducted on the fresh Zn-api-carbamate adduct (black trace) and the recycled species after the 2nd (red trace) and 5th (blue trace) independent catalytic cycles.